

The role of the S_3 GUT leptoquark in flavor universality and collider searches

Ilja Doršner^{a,c} Svjetlana Fajfer^{b,c} Darius A. Faroughy^c Nejc Košnik^{b,c}

^aUniversity of Split, Faculty of Electrical Engineering, Mechanical Engineering and Naval Architecture in Split (FESB), Ruđera Boškovića 32, 21000 Split, Croatia

^bDepartment of Physics, University of Ljubljana, Jadranska 19, 1000 Ljubljana, Slovenia

^cJ. Stefan Institute, Jamova 39, P. O. Box 3000, 1001 Ljubljana, Slovenia

E-mail: ilja.dorsner@ijs.si, svjetlana.fajfer@ijs.si,
nejc.kosnik@ijs.si, darius.faroughy@ijs.si

ABSTRACT: We investigate the ability of the S_3 scalar leptoquark to address the recent hints of lepton universality violation in B meson decays. The S_3 leptoquark with quantum numbers $(\mathbf{3}, \mathbf{3}, 1/3)$ naturally emerges in the context of an $SU(5)$ GUT model without any conflict with the stringent limits from observed nucleon stability. Scalar leptoquark S_3 with left-handed couplings to 2nd and 3rd generations of charged leptons and down-type quarks seems well-suited to address both $R_{K^{(*)}}$ and $R_{D^{(*)}}$. We quantify this suitability with numerical fits to a plethora of relevant flavor observables. The proposed $SU(5)$ model calls for a second leptoquark state, i.e., \tilde{R}_2 with quantum numbers $(\mathbf{3}, \mathbf{2}, 1/6)$, if one is to generate gauge coupling unification and neutrino mass. We accordingly include it in our study to investigate \tilde{R}_2 's ability to offset adverse effects of S_3 and thus improve a quality of numerical fits. A global fit of the leptoquark Yukawa couplings shows that large couplings of light S_3 to τ leptons are preferred. We furthermore identify $B \rightarrow K^{(*)}\bar{\nu}\nu$ as the most sensitive channel to probe the preferred region of parameter space. Large couplings of S_3 to τ leptons are finally confronted with the experimental searches for τ final states at the Large Hadron Collider. These searches comprise a study of decay products of the leptoquark pair production, as well as, and more importantly, an analysis of the high-mass $\tau\tau$ final states.

ARXIV EPRINT: [1711.07779](https://arxiv.org/abs/1711.07779)

Contents

1	Introduction	2
2	Model setup	3
3	LFU violating contributions	5
3.1	Charged currents LFU: $R_{D^{(*)}}$	5
3.2	Neutral currents: $R_{K^{(*)}}$, $\mathcal{B}(B \rightarrow K^{(*)}\mu^+\mu^-)$ and related observables	6
4	Constraints on the LQ couplings	7
4.1	LFU ratios and decay rates in charged currents	7
4.1.1	Semileptonic B decays	7
4.1.2	Semileptonic K and τ decays	7
4.1.3	Leptonic decays: $W \rightarrow \tau\bar{\nu}$, $\tau \rightarrow \ell\bar{\nu}\nu$	8
4.1.4	Semileptonic decays of D and t	9
4.2	LFV and neutral currents	9
4.2.1	$\tau \rightarrow \mu\gamma$	9
4.2.2	$Z \rightarrow \mu\tau$ and $\tau \rightarrow 3\mu$	9
4.2.3	$(g-2)_\mu$	10
4.2.4	$B \rightarrow K\mu\tau$ decays	10
4.2.5	$B_s-\bar{B}_s$ mixing frequency	10
4.2.6	$B \rightarrow K^{(*)}\nu\bar{\nu}$	12
4.2.7	$b\bar{b} \rightarrow \mu^+\mu^-$ scattering	13
4.2.8	D decays	13
5	Flavor couplings	13
5.1	S_3 coupled to muons (2 parameters)	14
5.2	S_3 coupled to muons and taus (4 parameters)	15
5.3	S_3 and \tilde{R}_2 (6 parameters)	16
6	Collider constrains	17
6.1	LQ pair production	17
6.2	High-mass $\tau\tau$ production	18
7	GUT completion	22
8	Conclusion	24
A	LQ pair production recast	25
B	High-mass $\tau\tau$ production cross-sections	26

1 Introduction

At low energies there are a few experimentally measured observables that exhibit deviation from the Standard Model (SM) predictions. Among them, the three B meson anomalies, indicating possible lepton flavor universality (LFU) violation, particularly stand out.

One of these anomalies manifests itself in the ratios

$$R_{D^{(*)}} = \frac{\Gamma(B \rightarrow D^{(*)}\tau^-\bar{\nu})}{\Gamma(B \rightarrow D^{(*)}\ell^-\bar{\nu})}, \quad (1.1)$$

according to the experimental results in Refs. [1–7]. The result for R_D appears to be 1.9σ larger than the SM prediction, i.e., $R_D^{\text{SM}} = 0.286 \pm 0.012$, that is obtained by relying on the lattice QCD results for both the vector and the scalar form factors [8] (see also Ref. [9]). The experimentally established $R_{D^*} = 0.304 \pm 0.020$ has also been confirmed [6, 7, 10], and it appears to be $\sim 3\sigma$ larger than predicted value $R_{D^*}^{\text{SM}} = 0.252 \pm 0.003$ [11]. The deviation from the SM prediction in the R_D – R_{D^*} plane is at 3.9σ level [10, 12, 13] and it has accordingly attracted a lot of attention recently [11, 14–20].

The remaining two B meson anomalies are related to the $b \rightarrow s\ell^+\ell^-$ transition. Namely, the LHCb experiment has found that there are slight discrepancies between the SM prediction and the experimental results for the angular observable known as P'_5 in $B \rightarrow K^*\mu^+\mu^-$ process. In many approaches this disagreement has been attributed to new physics (NP), although the tension might be a result of the SM QCD effects (see e.g. Ref. [21] and references therein). The second of the two $b \rightarrow s\ell^+\ell^-$ transition anomalies has been found in the ratio of the branching fractions,

$$\begin{aligned} R_K &\equiv \frac{\mathcal{B}(B^+ \rightarrow K^+\mu^+\mu^-)_{q^2 \in [1,6] \text{ GeV}^2}}{\mathcal{B}(B^+ \rightarrow K^+e^+e^-)_{q^2 \in [1,6] \text{ GeV}^2}} = 0.745 \pm_{0.074}^{0.090} \pm 0.036 \text{ [22]}, \\ R_{K^*}^{q^2 \in [1.1, 6] \text{ GeV}^2} &\equiv \frac{\mathcal{B}(B^0 \rightarrow K^{*0}\mu^+\mu^-)_{q^2 \in [1.1, 6] \text{ GeV}^2}}{\mathcal{B}(B^0 \rightarrow K^{*0}e^+e^-)_{q^2 \in [1.1, 6] \text{ GeV}^2}} = 0.69_{-0.07}^{+0.11} \pm 0.05 \text{ [23]}, \\ R_{K^*}^{q^2 \in [0.045, 1.1] \text{ GeV}^2} &= 0.66_{-0.07}^{+0.11} \pm 0.03 \text{ [23]}. \end{aligned} \quad (1.2)$$

The values the LHCb experiment measured for these ratios are consistently lower than the SM prediction, i.e., $R_K^{\text{SM}} = 1.00 \pm 0.03$, in which the next-to-next-to-leading QCD corrections and soft QED effects have been included [24, 25] (for R_{K^*} see Table 1 and references in [23]). In other words, the LHCb results point towards a significant effect of the lepton flavor universality violation in this process. Recently, Belle Collaboration [26] found out that the angular observable P'_5 agrees with the SM prediction much better for electrons than for muons. This important result suggests that it is much more likely that beyond the SM effects are present in the second generation of leptons, and that there are currently no effects in $b \rightarrow se^+e^-$ which would not be accounted for in the SM.

Many scenarios of NP [8, 16, 17, 27–49] have been investigated in order to explain either $R_{K^{(*)}}$ and P'_5 , or $R_{D^{(*)}}$ anomalies. An interesting observation was found in Ref. [17] that $R_{K^{(*)}}$ and P'_5 can be explained if NP couples only to the third generation of quarks and leptons. Furthermore, the authors of Refs. [32, 50] noticed that both $R_{D^{(*)}}$ and $R_{K^{(*)}}$

puzzles can be correlated if the effective four-fermion semileptonic operators consist of left-handed doublets.

In this work we consider a Grand Unified Theory (GUT) inspired setting with a light scalar S_3 leptoquark (LQ) that transforms as $(\bar{\mathbf{3}}, \mathbf{3}, 1/3)$ under the SM gauge group $SU(3) \times SU(2) \times U(1)$. The state S_3 is rendered baryon number conserving due to the GUT symmetry, as we discuss in Sec. 7, and generates purely left-handed current $\bar{L}L\bar{Q}Q$ operators which seem to be well-suited to explain the LFU puzzles if the S_3 mass is at the TeV scale. The need for the second light LQ state, \tilde{R}_2 in representation $(\mathbf{3}, \mathbf{2}, 1/6)$, emerges naturally from the requirement of neutrino masses generation in the advocated GUT model as well as from the gauge coupling unification. We accordingly include \tilde{R}_2 in our study and investigate whether it could partially compensate for the adverse low-energy effects of S_3 . In Sec. 2 we introduce relevant couplings of these two LQs with the SM fermions. We proceed to show how S_3 could, in principle, address the LFU puzzles in Sec. 3. We then present relevant additional constraints on the LQ parameters in Sec. 4. The low-energy flavor analysis is concluded in Sec. 5 with the global fit of the relevant couplings of the two LQs with quark-lepton pairs for three specific Yukawa structures. Sec. 6 is devoted to collider study of the model signatures in the LQ resonant pair production and in a t -channel LQ exchange contributing to $\tau\tau$ final states at LHC. We elaborate on the GUT construction behind the two LQ states in Sec. 7. Finally, we conclude in Sec. 8.

2 Model setup

The LQ multiplet $S_3(\bar{\mathbf{3}}, \mathbf{3}, 1/3)$ interacts with the SM fermions in accordance with its quantum numbers, given in the brackets. The three charge eigenstate components of S_3 , i.e., $S_3^{4/3}$, $S_3^{1/3}$, and $S_3^{-2/3}$, have the following Yukawa interactions with fermions [51]

$$\begin{aligned} \mathcal{L}_{S_3} = & -y_{ij}\bar{d}_L^C{}^i\nu_L^j S_3^{1/3} - \sqrt{2}y_{ij}\bar{d}_L^C{}^i e_L^j S_3^{4/3} + \\ & + \sqrt{2}(V^*y)_{ij}\bar{u}_L^C{}^i\nu_L^j S_3^{-2/3} - (V^*y)_{ij}\bar{u}_L^C{}^i e_L^j S_3^{1/3} + \text{h.c.}, \end{aligned} \quad (2.1)$$

where V is the Cabibbo-Kobayashi-Maskawa (CKM) mixing matrix. Note that S_3 has purely left-handed couplings. The diquark interactions with S_3 are not shown in Eq. (2.1) since we assume that S_3 and its interactions originate from the GUT construction presented in Ref. [52] where the baryon number violating diquark couplings are forbidden due to the grand unified symmetry.¹ The main goal of our study is to address the puzzles observed in neutral current LFU tests in the R_K ratio (and related anomalies in $b \rightarrow s\mu^+\mu^-$) as well as in charged-current LFU ratios $R_{D^{(*)}}$. Thus we have clear target observables that we can affect with a small number of LQ Yukawa couplings.

In the context of SM complemented with effective operators (SM-EFT) it has been shown that NP models contributing to dimension-6 operators made out of left-handed quark and lepton doublets can explain both neutral- and charged-current LFU anomalies [17, 32, 50, 53, 54]. However, in an explicit NP model these effective interactions could be correlated,

¹Complete model-independent sets of S_3 and \tilde{R}_2 couplings to fermions can be found in Ref. [51].

unlike in the effective theory², with other observables. Our intention is to quantify this correlation within this particular model.

The LQ state S_3 can affect all the target LFU observables with a minimal set of parameters, e.g., $y_{s\mu}$, $y_{b\mu}$, and $y_{b\tau}$. In this work, however, we also study the effect of the coupling $y_{s\tau}$ which enables a handle on the semitauonic modes entering $R_{D^{(*)}}$. The couplings of S_3 to d_L and e_L have to be rather small in order to avoid pressing bounds from LFV and kaon physics. We opt to set those couplings to zero to obtain the following flavor structure:

$$y = \begin{pmatrix} 0 & 0 & 0 \\ 0 & y_{s\mu} & y_{s\tau} \\ 0 & y_{b\mu} & y_{b\tau} \end{pmatrix}, \quad V^* y = \begin{pmatrix} 0 & V_{us}^* y_{s\mu} + V_{ub}^* y_{b\mu} & V_{us}^* y_{s\tau} + V_{ub}^* y_{b\tau} \\ 0 & V_{cs}^* y_{s\mu} + V_{cb}^* y_{b\mu} & V_{cs}^* y_{s\tau} + V_{cb}^* y_{b\tau} \\ 0 & V_{ts}^* y_{s\mu} + V_{tb}^* y_{b\mu} & V_{ts}^* y_{s\tau} + V_{tb}^* y_{b\tau} \end{pmatrix}. \quad (2.2)$$

Note that the Yukawa couplings of S_3 to up-type quarks are spread over generations due to CKM rotation. In what follows all Yukawa couplings are assumed to be real. The ansatz of Eq. (2.2) summarizes the most general S_3 scenario studied within our work, although we will also comment on more restricted scenarios, where some additional elements of y will be set to zero.

Having only one LQ with mass around the 1 TeV scale would invalidate unification of gauge couplings, thus a second LQ state — \tilde{R}_2 in our case — is needed. The two electric charge eigenstates of \tilde{R}_2 couple only to down-type quarks:

$$\mathcal{L}_{\tilde{R}_2} = -\tilde{y}_{ij} \bar{d}_R^i e_L^j \tilde{R}_2^{2/3} + \tilde{y}_{ij} \bar{d}_R^i \nu_L^j \tilde{R}_2^{-1/3} + \text{h.c.} \quad (2.3)$$

The doublet \tilde{R}_2 can accommodate the measured value of R_K , but its right-handed current contributions cause tensions with the reported value for R_{K^*} . In the current setting with strictly left-handed neutrinos \tilde{R}_2 does not interact with up-type quarks and thus cannot affect $R_{D^{(*)}}$. In our approach it is S_3 that could, in principle, address both LFU anomalies, whereas its side-effects in other well-constrained observables (e.g. $B_s - \bar{B}_s$ mixing and $B \rightarrow K^{(*)} \bar{\nu} \nu$) might be, hopefully, cancelled by \tilde{R}_2 . Since S_3 will have largest effects in the τ sector we have to introduce couplings of \tilde{R}_2 to τ in order to compensate for potentially unwanted effects. In the following analysis we will analyze a light S_3 scenario with the couplings texture (2.2) and along with it test the viability of having light \tilde{R}_2 with nonzero Yukawas involving the τ lepton. Namely, we take

$$\tilde{y} = \begin{pmatrix} 0 & 0 & 0 \\ 0 & 0 & \tilde{y}_{s\tau} \\ 0 & 0 & \tilde{y}_{b\tau} \end{pmatrix}. \quad (2.4)$$

The mass of \tilde{R}_2 should be at around 1 TeV in order to affect low-energy phenomenology, if required at all. We consistently take this to be the case when we discuss the role of \tilde{R}_2 in gauge coupling unification and the neutrino mass generation.

²Even in the effective theory the quantum corrections have strong effect on low-energy precision measurements [54, 55].

For both LQ states the rotations with the CKM matrix V , left over from the transition to the mass basis of fermions, have been assigned to the u_L fields. For the study of flavor phenomenology the neutrinos can be safely considered as massless. Thus, Lagrangians in Eqs. (2.1) and (2.3) are written in the fermion mass basis with the exception of ν_L whose mass basis is ill-defined. We use flavor basis for the neutrinos, such that the Pontecorvo-Maki-Nakagawa-Sakata (PMNS) matrix becomes unity.

3 LFU violating contributions

In this section we focus on how the two light LQs would affect the LFU violating anomalies measured in B meson decays. The gross features required of Yukawa matrices will be presented. The detailed discussion of additional observables and their interplay with the LFU anomalies will be presented in the next section.

3.1 Charged currents LFU: $R_{D^{(*)}}$

The largest LFU violating effect is in the charged current observables $R_{D^{(*)}}$. For a NP-induced effective operator that follows the chirality structure of the SM it has been shown that the dimensionless coupling of ~ 0.1 is needed, if new particles have mass of $\Lambda = 1$ TeV and contribute at tree level [41]. The matched contributions of S_3 generate left-handed current operator, whereas \tilde{R}_2 cannot contribute to charged currents in this setup³. In particular in $b \rightarrow c\ell\bar{\nu}$ transition the S_3 presence leads to the modification of the left-handed charged-current operators:

$$\mathcal{L}_{\text{SL}} = -\frac{4G_F}{\sqrt{2}} \left[(V_{UD} + g_{UD;\ell\ell}^L)(\bar{U}\gamma^\mu P_L D)(\bar{\ell}\gamma_\mu P_L \nu_\ell) \right], \quad U = u, c, t, \quad D = s, b, \quad \ell = \mu, \tau, \quad (3.1)$$

where the LQ term in Eq. (3.1) reads

$$g_{UD;\ell\nu}^L = -\frac{v^2}{4m_{S_3}^2} (Vy^*)_{U\ell} y_{D\nu}. \quad (3.2)$$

The effect of S_3 may be also understood as nonuniversal CKM elements in semileptonic charged-current processes:

$$|V_{ij}^{(\ell)}|^2 = |V_{ij}|^2 \left[1 - \frac{v^2}{2m_{S_3}^2} \text{Re} \left(\frac{V_{is}}{V_{ij}} y_{s\ell}^* y_{j\ell} + \frac{V_{ib}}{V_{ij}} y_{b\ell}^* y_{j\ell} \right) \right], \quad i = u, c, t, \quad j = s, b, \quad \ell = \mu, \tau. \quad (3.3)$$

One also has lepton flavor violating S_3 contributions parameterized by $g_{UD;\ell\nu}$, with their effect being much smaller since they do not interfere with the SM amplitude. They contribute at subleading order, namely at $v^4/m_{S_3}^4$ that we neglect in comparison to the interference terms. Here $v = 246$ GeV is the electroweak vacuum expectation value. Notice that the form of interaction imposed in Eq. (2.2) implies that both decay modes $B \rightarrow D^{(*)}\tau\nu_\tau$ and

³Charged currents can be induced by \tilde{R}_2 if right-handed neutrinos are added to the fermion sector.

$B \rightarrow D^{(*)} \mu \nu_\mu$ are affected. From the fit to the measured ratio $R_{D^{(*)}}$, performed in Ref. [41], we learn that at 1σ we have the following constraint on the S_3 Yukawas:

$$\text{Re} [V_{cb} (|y_{b\tau}|^2 - |y_{b\mu}|^2) + V_{cs} (y_{b\tau} y_{s\tau}^* - y_{b\mu} y_{s\mu}^*)] = -2C_{V_L} (m_{S_3}/\text{TeV})^2, \quad C_{V_L} = 0.18 \pm 0.04. \quad (3.4)$$

The $R_{D^{(*)}}$ constraint of Eq. (3.4) includes effects from $\tau \bar{\nu}_\tau$ and $\mu \bar{\nu}_\mu$ states. It is important to notice definite signs of the LQ-SM interference contributions which are proportional to V_{cb} . Large $y_{b\tau}$ is clearly disfavoured by (3.4) while $y_{b\mu}$ results in negative interference term in semi-muonic modes that would be welcome from the $R_{D^{(*)}}$ point of view, however this possibility could be in conflict with precise measurements of LFU in $R_{D^{(*)}}^{\mu/e}$ (studied below in Sec. 4). Out of the remaining two terms $y_{b\mu} y_{s\mu}^*$ is negligible in Eq.(3.4) as required by the $b \rightarrow s\mu^+\mu^-$. The only numerical scenario with positive interference term for the semi-tauonic mode is the one with large Cabibbo favored contribution,

$$y_{b\tau} y_{s\tau}^* \approx -0.4(m_{S_3}/\text{TeV})^2. \quad (3.5)$$

In the next section we will introduce constraints that put important bound on the above product of Yukawas.

3.2 Neutral currents: $R_{K^{(*)}}$, $\mathcal{B}(B \rightarrow K^{(*)} \mu^+ \mu^-)$ and related observables

The R_K anomaly can be accounted for by the additional contribution of S_3 state to the effective four-Fermi operators that are a product of left-handed quark and lepton currents [51]. The \tilde{R}_2 state alone can also explain R_K via the right-handed current operators [56], but the recent measurement of R_{K^*} being significantly smaller than 1 [23] implies that these operators' contributions must be small [29, 56]. If we expand our analysis to a whole family of observables driven by $b \rightarrow s\mu^+\mu^-$ process the scenario with left-handed currents (S_3 state) presents a good fit and prefers the following range at 1σ [49] (see also [53, 57]):

$$C_9 = -C_{10} = -0.61_{-0.10}^{+0.13}. \quad (3.6)$$

The exchange of $S_3^{4/3}$ contributes towards the above effective coefficients as

$$C_9 = -C_{10} = \frac{\pi}{V_{tb} V_{ts}^* \alpha} y_{b\mu} y_{s\mu}^* \frac{v^2}{m_{S_3}^2}. \quad (3.7)$$

For a range (3.6) of Wilson coefficients we find

$$y_{b\mu} y_{s\mu}^* = (-0.958_{-0.020}^{+0.016}) \times 10^{-3} (m_{S_3}/\text{TeV})^2. \quad (3.8)$$

Contrary to S_3 , the right-handed quark currents generated by \tilde{R}_2 do not improve significantly the global agreement between theory predictions and observables related to the $b \rightarrow s\mu^+\mu^-$. Tree-level matching of \tilde{R}_2 amplitudes yields

$$C'_9 = -C'_{10} = -\frac{\pi}{V_{tb} V_{ts}^* \alpha} \tilde{y}_{s\mu} \tilde{y}_{b\mu}^* \frac{v^2}{m_{\tilde{R}_2}^2}. \quad (3.9)$$

Using the result of the global fit from [49] we have checked that including non-zero $\tilde{y}_{s\mu}$ and $\tilde{y}_{b\mu}$ does not improve the fit considerably.

4 Constraints on the LQ couplings

The introduction of the two LQ states with sizable couplings to explain the LFU observables, as presented above, inevitably causes side effects in related flavor observables which we will focus on in this section.

4.1 LFU ratios and decay rates in charged currents

4.1.1 Semileptonic B decays

Besides measuring $R_{D^{(*)}}$ that does not distinguish between e and μ in the final state, Belle Collaboration also reported on the lepton universality ratio in e and μ . Here we will use $R_{D^*}^{e/\mu} = 1.04(5)(1)$ [58] and $R_D^{\mu/e} = 0.995(22)(39)$ [59], both of which are consistent with 1. In our framework the S_3 state can potentially contribute to those ratios by rescaling the overall normalization of $B \rightarrow D^{(*)}\mu\nu$. It follows from Eq. (3.3) that the S_3 contributions in these decays are constrained:

$$-\frac{v^2}{2m_{S_3}^2} \text{Re} \left[\left(\frac{V_{cs}}{V_{cb}} y_{s\mu}^* + y_{b\mu}^* \right) y_{b\mu} \right] = R_{D^{(*)}}^{\mu/e} - 1 = -0.023 \pm 0.043, \quad (4.1)$$

where we have averaged over the two Belle results. Due to its smallness the term $y_{s\mu} y_{b\mu}^*$ is irrelevant in the above equation (see Eq. (3.8)), albeit the factor ~ 20 enhancement due to CKM. After this simplification Eq. (4.1) becomes a rather weak limit, i.e., $|y_{b\mu}| \lesssim 1.5(m_{S_3}/\text{TeV})$. It is, however, clear that $y_{b\mu}$, in spite of its large value, is not sufficient to explain the $R_{D^{(*)}}$ constraint of Eq. (3.4). Since the largest effects are concentrated in the τ flavor, we expect large effect in leptonic decay of $B^- \rightarrow \tau\bar{\nu}$ which is sensitive to $|V_{ub}^{(\tau)}|^2 \approx |V_{ub}|^2 [1 - v^2/(2m_{S_3}^2) \text{Re}((V_{us}/V_{ub})y_{s\tau}^* y_{b\tau})]$, as given in Eq. (3.3). The $B^- \rightarrow \tau\bar{\nu}$ rate is thus enhanced by the same combination of Yukawas (and same order of Cabibbo angle) that also drives the $B \rightarrow D^{(*)}\tau\bar{\nu}$ rate. The current experimental average $\mathcal{B}(B^- \rightarrow \tau\bar{\nu}) = (1.09 \pm 0.24) \times 10^{-4}$ is indeed slightly higher than the SM prediction $\mathcal{B}(B^- \rightarrow \tau\bar{\nu})^{\text{SM}} = (0.78 \pm 0.07) \times 10^{-4}$. If we assume that LQ Yukawas are real numbers then the leading contribution $y_{s\tau}^* y_{b\tau}$ in both observables leads to correlation

$$\frac{\mathcal{B}(B^- \rightarrow \tau\bar{\nu})}{\mathcal{B}(B^- \rightarrow \tau\bar{\nu})^{\text{SM}}} - 1 \approx \left(\frac{R_{D^{(*)}}}{R_{D^{(*)}}^{\text{SM}}} - 1 \right) \frac{\rho}{\rho^2 + \eta^2}, \quad (4.2)$$

where the CKM factor relating the two observables is close to unity.

4.1.2 Semileptonic K and τ decays

On the other hand, LFU in kaon decays has been tested and confirmed with better precision through the following ratios:

$$R_{e/\mu}^K = \frac{\Gamma(K^- \rightarrow e^- \bar{\nu})}{\Gamma(K^- \rightarrow \mu^- \bar{\nu})}, \quad R_{\tau/\mu}^K = \frac{\Gamma(\tau^- \rightarrow K^- \nu)}{\Gamma(K^- \rightarrow \mu^- \bar{\nu})}. \quad (4.3)$$

As pointed out in Ref. [42] these observables enable us to put strong constraints on the corrections arising within models of NP. In the e/μ sector the experimental result [60] agrees well with the SM prediction [61]:

$$R_{e/\mu}^{K(\text{exp})} = (2.488 \pm 0.010) \times 10^{-5}, \quad R_{e/\mu}^{K(\text{SM})} = (2.477 \pm 0.001) \times 10^{-5}. \quad (4.4)$$

Using Eq. (3.3) we recast Eq. (4.4):

$$\frac{R_{e/\mu}^{K(\text{exp})}}{R_{e/\mu}^{K(\text{SM})}} - 1 = \frac{v^2}{2m_{S_3}^2} \text{Re} [|y_{s\mu}|^2 + (V_{ub}/V_{us})y_{b\mu}^*y_{s\mu}] = (4.4 \pm 4.0) \times 10^{-3} \quad (4.5)$$

$$\Rightarrow |y_{s\mu}| \lesssim 0.5(m_{S_3}/\text{TeV}).$$

$R_{e/\mu}^K$ is most sensitive to $|y_{s\mu}|$ since the product $y_{b\mu}^*y_{s\mu}$ must be small as dictated by $b \rightarrow s\mu\mu$ sector and comes with an additional CKM suppression. The agreement of experiment [60] with the SM prediction [62] in the τ/μ exhibits a $\sim 2\sigma$ tension:

$$R_{\tau/\mu}^{K(\text{exp})} = 467.0 \pm 6.7, \quad R_{\tau/\mu}^{K(\text{SM})} = \frac{m_K^3(m_\tau^2 - m_K^2)^2}{2m_\tau m_\mu^2(m_K^2 - m_\mu^2)^2} (1 + \delta R_{\tau/K}) = 480.3 \pm 1.0, \quad (4.6)$$

where the dominant error of the experimental ratio is due to the τ lifetime uncertainty, whereas on the theory side it is the radiative correction $\delta R_{\tau/K} = (0.90 \pm 0.22)\%$ [63] which is the source of uncertainty. The constraint is expressed as:

$$\frac{R_{\tau/\mu}^{K(\text{exp})}}{R_{\tau/\mu}^{K(\text{SM})}} - 1 = \frac{v^2}{2m_{S_3}^2} \text{Re} [|y_{s\mu}|^2 - |y_{s\tau}|^2 + (V_{ub}/V_{us})(y_{b\mu}^*y_{s\mu} - y_{b\tau}^*y_{s\tau})] = (-2.8 \pm 1.4) \times 10^{-2}. \quad (4.7)$$

4.1.3 Leptonic decays: $W \rightarrow \tau\bar{\nu}$, $\tau \rightarrow \ell\bar{\nu}\nu$

The SM tree-level vertex $\bar{\nu}\nu W$ is rescaled due to penguin-like contribution of both S_3 and \tilde{R}_2 . As we integrate out S_3 and \tilde{R}_2 at the weak scale the W vertex with τ leptons reads $\frac{-g}{\sqrt{2}}\bar{\nu}_\tau \tilde{W} P_L \tau (1 + \delta_W^{(\tau)})$, where

$$\delta_W^{(\tau)} = \frac{N_c}{288\pi^2} [(2x + 6x \log x - 6x\pi i) (|y_{b\tau}|^2 + |y_{s\tau}|^2) + \tilde{x} (|\tilde{y}_{s\tau}|^2 + |\tilde{y}_{b\tau}|^2)],$$

$$x = \frac{m_W^2}{m_{S_3}^2}, \quad \tilde{x} = \frac{m_W^2}{m_{\tilde{R}_2}^2}. \quad (4.8)$$

Free color index in the loops graphs results in the $N_c = 3$ factor in front. We have neglected the quark masses in the above calculation and presented only the leading terms in x and \tilde{x} . The contribution of S_3 with mass of 1 TeV shifts the $W \rightarrow \tau\nu$ decay width relatively by $4 \times 10^{-4}(|y_{b\tau}|^2 + |y_{s\tau}|^2)$ which is well below the current $\sim 2\%$ experimental precision. The $W \rightarrow \mu\bar{\nu}$ is also rescaled by an analogous $\delta_W^{(\mu)}$ factor.

At low energies the effective $W \rightarrow \tau\nu$ vertex would, together with direct box contributions with LQs, manifest itself in the $\tau \rightarrow \ell\bar{\nu}_\ell\bar{\nu}_\tau$ decays. Only S_3 may participate in the box diagrams since \tilde{R}_2 has no direct couplings to ℓ . The effective interaction term of $\tau \rightarrow \ell\nu_\tau\bar{\nu}_\ell$ then reads $\frac{-g^2}{2m_W^2}(\bar{\nu}_\tau\gamma_\mu P_L \tau)(\bar{\ell}\gamma^\mu P_L \ell)[1 + \delta_W^{(\tau)} + \delta_W^{(\ell)} + \delta_{\tau\ell\nu\nu}^{\text{box}}]$, with

$$\delta_{\tau\ell\nu\nu}^{\text{box}} = \frac{N_c}{128\pi^2} \frac{v^2}{m_{S_3}^2} [(y^\dagger y)_{\ell\tau}^2 + 4(y^\dagger y)_{\tau\tau}(y^\dagger y)_{\ell\ell}]. \quad (4.9)$$

As it has been pointed out recently in the literature [54, 55, 62] the LFU observable $R_\tau^{\tau/\ell}$, defined as a ratio $\mathcal{B}(\tau \rightarrow \ell\nu\nu)/\mathcal{B}(\mu \rightarrow e\nu\nu)$, and normalized to the SM prediction of this

ratio, is very sensitive to models modifying couplings of the τ lepton. Experimentally, $R_\tau^{\tau/\mu} = 1.0022 \pm 0.0030$, $R_\tau^{\tau/e} = 1.0060 \pm 0.0030$, while in the present model the leading interference terms shift the ratios as

$$R_\tau^{\tau/e} = 1 + 2\text{Re}\left(\delta_W^{(\tau)} - \delta_W^{(\mu)}\right), \quad R_\tau^{\tau/\mu} = 1 + 2\text{Re}\left(\delta_W^{(\tau)} + \delta_{\tau\mu\nu\nu}^{\text{box}}\right). \quad (4.10)$$

4.1.4 Semileptonic decays of D and t

We have checked the effect of S_3 on the leptonic charm meson decays $D_s \rightarrow \ell\nu$. Using the bounds from kaon LFU observables presented above we find that the S_3 correction to the $D \rightarrow \mu\nu$ width is below 1%, while the experimental uncertainty of $D_s \rightarrow \tau\nu$ is 4% and can easily accommodate $|y_{s\tau}| \lesssim 1.2(m_{S_3}/\text{TeV})$ without even taking into account the uncertainty in the decay constant f_{D_s} . For the semileptonic top decay process among the third generation fermions, $t \rightarrow b\tau^+\nu$, the correction is also below the current sensitivity [64].

4.2 LFV and neutral currents

4.2.1 $\tau \rightarrow \mu\gamma$

Current bound $\mathcal{B}(\tau \rightarrow \mu\gamma) \leq 4.4 \times 10^{-8}$ has been determined by the BABAR collaboration [65]. The S_3 LQ contributes to the $\tau \rightarrow \mu\gamma$ amplitude via b and s quarks and $S_3^{4/3}$ in the loop and also via up quarks u , c , and t mediated by the $S_3^{-1/3}$ component. Using the loop functions in the small quark mass limit as in Ref. [51] we determine

$$\mathcal{L}_{\text{eff}}^{\tau \rightarrow \mu\gamma} = \frac{e}{2} \sigma_L^{\tau\mu} \bar{\mu}(i\sigma^{\mu\nu} P_L)\tau F_{\mu\nu}, \quad (4.11)$$

where the effective coupling reads

$$\sigma_L^{\tau\mu} = \frac{3m_\tau}{64\pi^2 m_{S_3}^2} [5y_{s\mu}y_{s\tau}^* + y_{b\mu}y_{b\tau}^*]. \quad (4.12)$$

4.2.2 $Z \rightarrow \mu\tau$ and $\tau \rightarrow 3\mu$

At loop level, S_3 and \tilde{R}_2 modify the $Z \rightarrow f_1\bar{f}_2$ decay widths which were precisely measured at LEP-2. The largest effects in presented LQ model are expected for third generation final states both in flavor conserving decays, as in $Z \rightarrow \tau^+\tau^-$, which has been shown to have only weak constraining power in Ref. [66], as well as in LFV modes $Z \rightarrow \tau^\pm\mu^\mp$. The latter decay happens due to penguin diagrams with S_3 as well as 1-particle reducible diagrams and is suppressed by a loop factor and small ratio $x = m_Z^2/m_{S_3}^2$, in which we expand to leading order:

$$\Gamma_{Z \rightarrow \tau^\mp\mu^\pm} = \frac{\sqrt{2}G_F m_Z^3}{3\pi} \left| \frac{N_c}{288\pi^2} x(2 - 3\cos^2\theta_W - 3\log x + 3\pi i) \right|^2 (|y_{s\mu}y_{s\tau}|^2 + y_{b\mu}y_{b\tau}|^2). \quad (4.13)$$

We have checked that $\mathcal{B}(Z \rightarrow \mu\tau)$ is well below the current experimental bound at 10^{-5} . Compared to the closely related $\tau \rightarrow \mu\gamma$ decay, this channel is less stringently constrained and thus we do not include it in the fit. On the other hand, the $\mathcal{B}(\tau \rightarrow 3\mu) < 2.1 \times 10^{-8}$ at 90% C.L. [60], and can be mediated by the above mentioned LFV Z vertex or via box

diagram containing S_3 and quarks. They are both encompassed in the low-energy effective Lagrangian:

$$\begin{aligned} \mathcal{L}_{\tau \rightarrow 3\mu} = & \frac{-N_c(y^\dagger y)_{\mu\tau}}{(4\pi)^2 m_{S_3}^2} \left[(y^\dagger y)_{\mu\mu} + \frac{\sqrt{2}}{9} G_F m_W^2 (2 - 3 \cos^2 \theta_W - 3 \log x - 3\pi i) \right] (\bar{\mu} \gamma^\mu P_L \tau) (\bar{\mu} \gamma_\mu P_L \mu) \\ & \frac{-N_c(y^\dagger y)_{\mu\tau}}{(4\pi)^2 m_{S_3}^2} \frac{2\sqrt{2}}{9} G_F m_Z^2 \sin^2 \theta_W (2 - 3 \cos^2 \theta_W - 3 \log x - 3\pi i) (\bar{\mu} \gamma^\mu P_L \tau) (\bar{\mu} \gamma_\mu P_R \mu), \end{aligned} \quad (4.14)$$

where, again, $x = m_Z^2/m_{S_3}^2$. The mixed chirality stems from the Z coupling to $\bar{\mu}_R \mu_R$. In the limit of $m_\mu/m_\tau \rightarrow 0$ the two terms above do not interfere. We notice that when all couplings are ~ 1 and $m_{S_3} = 1$ TeV then the $\mathcal{B}(\tau \rightarrow 3\mu)$ is in the ballpark of current experimental upper bound. As will be shown in Sec. 5, realistic values of the Yukawas result in much smaller contribution to this channel, and that is why we omit this channel from the fit.

4.2.3 $(g-2)_\mu$

The difference between the experimental value and the one predicted by the SM is $\delta a_\mu = a_\mu^{\text{exp}} - a_\mu^{\text{SM}} = (2.8 \pm 0.9) \times 10^{-9}$ [60]. Following [51] and using the Lagrangian of Eq. (2.1), we derive the contribution of S_3 to the muon anomalous magnetic moment:

$$\delta a_\mu^{S_3} = -\frac{3m_\mu^2}{(32\pi^2 m_{S_3}^2)} (|y_{s\mu}|^2 + |y_{b\mu}|^2). \quad (4.15)$$

Since the above contribution has wrong sign with respect to the experimental pull individual Yukawa couplings of S_3 to the μ should be small. Notice that the contribution of \tilde{R}_2 to $(g-2)_\mu$ is greatly suppressed and vanishes at $m_{s,b}/m_{\tilde{R}_2} \rightarrow 0$ [51, 67].

4.2.4 $B \rightarrow K\mu\tau$ decays

The lepton flavor violation can be induced by the LQ presence at tree level in $B \rightarrow K\mu\tau$ and also in decays of bottomonium to $\tau\mu$. As noticed in [42] the latter process has been constrained at the level of 10^{-6} however these bounds are not competitive with the bound $\mathcal{B}(B^- \rightarrow K^- \mu^\pm \tau^\mp) < 4.8 \times 10^{-5}$ at 90% C.L. [68]. This inclusive mode is sensitive to both $y_{s\tau} y_{b\mu}$ and $y_{s\mu} y_{b\tau}$ as $\mathcal{B}(B^- \rightarrow K^- \mu^\pm \tau^\mp) = 8.6 \times 10^{-3} [(y_{s\tau} y_{b\mu})^2 + (y_{s\mu} y_{b\tau})^2]$ when the form factors of Ref. [69] are used. The constraint then reads

$$\sqrt{(y_{b\tau} y_{s\mu})^2 + (y_{b\mu} y_{s\tau})^2} \lesssim 0.075 (m_{S_3}/\text{TeV})^2. \quad (4.16)$$

4.2.5 $B_s - \bar{B}_s$ mixing frequency

Despite being a loop observable in the LQ scenarios, the B_s meson mixing frequency is one of the most important constraints in our particular setup where the product of S_3 Yukawas $y_{b\tau} y_{s\tau}$ is large. This product alone would lead to uncomfortably large effect in the $B_s - \bar{B}_s$ oscillation frequency Δm_s . However, there is an additional box amplitude due to \tilde{R}_2 as well as an amplitude with both S_3 and \tilde{R}_2 propagating in the box, as shown

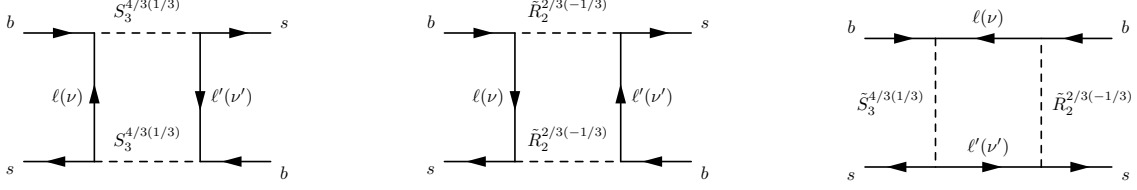


Figure 1. Three types of box-diagrams with S_3 and \tilde{R}_2 contributing to Δm_s .

in Fig. 1. Amplitudes that correspond to the first and second diagram in Fig. 1 can be found in Refs. [8, 51] and contribute to operators C_1 and \tilde{C}_1 of the effective Hamiltonian, respectively:

$$\mathcal{H}_{\Delta m_s} = (C_1^{\text{SM}} + C_1^{S_3}) (\bar{s}_L \gamma^\nu b_L)^2 + \tilde{C}_1^{\tilde{R}_2} (\bar{s}_R \gamma^\nu b_R)^2 + C_4^{S_3 \tilde{R}_2} (\bar{s}_R b_L) (\bar{s}_L b_R) + C_5^{S_3 \tilde{R}_2} (\bar{s}_R^\alpha b_L^\beta) (\bar{s}_L^\beta b_R^\alpha). \quad (4.17)$$

The third diagram in Fig. 1 in which both LQs are present, but couple with opposite chirality to the fermions, contributes to the Wilson coefficient C_5 . There the color indices α and β are summed across $\Delta B = 1$ currents. The box diagrams in Fig. 1 are well approximated using a limit of massless virtual leptons and match onto the effective Hamiltonian at scale $\Lambda = \mathcal{O}(m_{S_3}) \sim 1 \text{ TeV}$:

$$\begin{aligned} C_1^{\text{SM}}(m_t) &= \frac{m_W^2 S_0(x_t) (V_{tb} V_{ts}^*)^2}{8\pi^2 v^4}, \\ C_1^{S_3}(\Lambda) &= \frac{3(y y^\dagger)_{bs}^2}{128\pi^2 m_{S_3}^2}, \\ \tilde{C}_1^{\tilde{R}_2}(\Lambda) &= \frac{(\tilde{y} \tilde{y}^\dagger)_{sb}^2}{64\pi^2 m_{\tilde{R}_2}^2}, \\ C_4^{S_3 \tilde{R}_2}(\Lambda) &= 0, \\ C_5^{S_3 \tilde{R}_2}(\Lambda) &= \frac{(y y^\dagger)_{bb} (\tilde{y} \tilde{y}^\dagger)_{ss}}{16\pi^2} \frac{\log m_{S_3}^2 / m_{\tilde{R}_2}^2}{m_{S_3}^2 - m_{\tilde{R}_2}^2}. \end{aligned} \quad (4.18)$$

Evaluation of hadronic matrix elements for $B_s - \bar{B}_s$ mixing is performed at the scale $\mu = \bar{m}_b(\bar{m}_b) = 4.2 \text{ GeV}$. Utilizing parameterization in terms of bag parameters as in Ref. [70], we find for the oscillation frequency

$$\begin{aligned} \Delta m_s &= \frac{2}{3} m_{B_s} f_{B_s}^2 B_{B_s}^{(1)}(\mu) |C_1^{\text{SM}}(\mu)| \\ &\times \left| 1 + \left[\frac{C_1^{S_3} + \tilde{C}_1^{\tilde{R}_2}}{C_1^{\text{SM}}} \right]_\mu + \frac{1}{2} \left[\left(\frac{m_{B_s}}{\bar{m}_b(\bar{m}_b) + \bar{m}_s(\bar{m}_b)} \right)^2 + \frac{3}{2} \right] \left[\frac{B_{B_s}^{(5)} C_5^{\tilde{R}_2 S_3}}{B_{B_s}^{(1)} C_1^{\text{SM}}} \right]_\mu \right. \\ &\quad \left. + \frac{3}{2} \left[\left(\frac{m_{B_s}}{\bar{m}_b(\bar{m}_b) + \bar{m}_s(\bar{m}_b)} \right)^2 + \frac{1}{6} \right] \left[\frac{B_{B_s}^{(4)} C_4^{\tilde{R}_2 S_3}}{B_{B_s}^{(1)} C_1^{\text{SM}}} \right]_\mu \right|. \end{aligned} \quad (4.19)$$

For the SM prediction we use the perturbative QCD renormalization at next-to-leading order whose effect is subsumed in $\eta_{2B} = 0.55(1)$ [71]. The non-perturbative parameters

and perturbative RG running effects of C_1 are combined into a scale-invariant combination,

$$f_{B_s}^2 B_{B_s}^{(1)}(\mu) C_1^{\text{SM}}(\mu) = f_{B_s}^2 \hat{B}_{B_s}^{(1)} \eta_{2B} C_1^{\text{SM}}(m_t), \quad (4.20)$$

where the value of renormalization-group invariant bag parameter is taken from the QCD lattice simulation with three dynamical quarks [72]: $f_{B_s}^2 \hat{B}_{B_s}^{(1)} = 0.0754(46)(15) \text{ GeV}^2$ ⁴. First number in the brackets represents statistical and systematic error, apart from systematic error due to omission of dynamical charm-quark, which is shown in the second bracket. The SM prediction is then $\Delta m_s^{\text{SM}} = (19.6 \pm 1.6) \text{ ps}^{-1}$. For the LQ contributions in Eq. (4.19) we use the values of $B_{B_s}^{(i)}(\mu)$ from Ref. [72]. For the multiplicative renormalization of coefficients $C_1^{S_3}$ and $\tilde{C}_1^{\tilde{R}_2}$ we neglect the running from Λ to m_t , such that running effect to low scale is the same as in the SM, whereas for $C_{4,5}^{\tilde{R}_2 S_3}$ we use the leading order mixing [74] to find $C_4^{\tilde{R}_2 S_3}(\mu) = 0.61 C_5^{\tilde{R}_2 S_3}(\Lambda)$, $C_5^{\tilde{R}_2 S_3}(\mu) = 0.88 C_5^{\tilde{R}_2 S_3}(\Lambda)$. For the ratios of bag parameters we use central values to find $B_{B_s}^{(5)}(\mu)/B_{B_s}^{(1)}(\mu) = 0.99$, $B_{B_s}^{(4)}(\mu)/B_{B_s}^{(1)}(\mu) = 1.07$ [72]. Note that in this case the experimental value $\Delta m_s^{\text{exp}} = (17.757 \pm 0.021) \text{ ps}^{-1}$ has negligible uncertainty [60].

4.2.6 $B \rightarrow K^{(*)} \nu \bar{\nu}$

The $B \rightarrow K^{(*)} \nu \bar{\nu}$ decay offers an excellent probe of the lepton flavor conserving as well as lepton flavor violating combination of the LQ couplings. Following [42] and with the help of notation in Refs. [56, 75, 76], we write the effective Lagrangian:

$$\mathcal{L}_{\text{eff}}^{b \rightarrow s \bar{\nu} \nu} = \frac{G_F \alpha}{\pi \sqrt{2}} V_{tb} V_{ts}^* \left(\bar{s} \gamma_\mu [C_L^{ij} P_L + C_R^{ij} P_R] b \right) (\bar{\nu}_i \gamma^\mu (1 - \gamma_5) \nu_j). \quad (4.21)$$

In the SM we have a contribution for each pair of neutrinos and therefore $C_L^{\text{SM},ij} = C_L^{\text{SM}} \delta_{ij}$ where $C_L^{\text{SM}} = -6.38 \pm 0.06$ [75]. The respective contributions of S_3 and \tilde{R}_2 to the left- and right-handed operators are [51]:

$$C_L^{S_3,ij} = \frac{\pi v^2}{2\alpha V_{tb} V_{ts}^* m_{S_3}^2} y_{bj} y_{si}^*, \quad C_R^{\tilde{R}_2,ij} = -\frac{\pi v^2}{2\alpha V_{tb} V_{ts}^* m_{\tilde{R}_2}^2} \tilde{y}_{sj} \tilde{y}_{bi}^*. \quad (4.22)$$

While the amplitude of $B \rightarrow K \bar{\nu} \nu$ depends only on the vectorial part of Wilson coefficients (4.22), the $B \rightarrow K^* \bar{\nu} \nu$ amplitude is also sensitive to axial current, and the two decay modes constrain the right-handed Wilson coefficient differently. We follow Ref. [76] and introduce

$$\epsilon_{ij} = \frac{\sqrt{|C_L^{\text{SM}} \delta_{ij} + C_L^{S_3,ij}|^2 + |C_R^{\tilde{R}_2,ij}|^2}}{|C_L^{\text{SM}}|}, \quad \eta_{ij} = \frac{-\text{Re} \left[(C_L^{\text{SM}} \delta_{ij} + C_L^{S_3,ij}) C_R^{\tilde{R}_2,ij*} \right]}{|C_L^{\text{SM}} \delta_{ij} + C_L^{S_3,ij}|^2 + |C_R^{\tilde{R}_2,ij}|^2}. \quad (4.23)$$

⁴We prefer to use the results of Ref. [72] that include bag parameters for the whole operator basis. However, for $B_{B_s}^{(1)}$ we have found good agreement with the FLAG average of 2+1 dynamical simulations, $f_{B_s}^2 \hat{B}_{B_s}^{(1)} = 0.0729(86)$ [73].

Then the SM-normalized branching fractions are

$$\begin{aligned}
R_{\nu\nu} &= \frac{\mathcal{B}(B \rightarrow K\bar{\nu}\nu)}{\mathcal{B}(B \rightarrow K\bar{\nu}\nu)_{\text{SM}}} = \frac{1}{3} \sum_{ij} (1 - 2\eta_{ij}) \epsilon_{ij}^2, \\
R_{\nu\nu}^* &= \frac{\mathcal{B}(B \rightarrow K^*\bar{\nu}\nu)}{\mathcal{B}(B \rightarrow K^*\bar{\nu}\nu)_{\text{SM}}} = \frac{1}{3} \sum_{ij} (1 + \kappa_\eta \eta_{ij}) \epsilon_{ij}^2,
\end{aligned}
\tag{4.24}$$

where $\kappa_\eta = 1.34 \pm 0.04$ [76]. Among the possible final states, we will take the two strongest bounds on $R_{\nu\nu}^{(*)}$ determined by the Belle experiment, $\mathcal{B}(B \rightarrow K^*\bar{\nu}\nu) < 2.7 \times 10^{-5}$ and $\mathcal{B}(B \rightarrow K\bar{\nu}\nu) < 1.6 \times 10^{-5}$ which translate to $R_{\nu\nu}^* < 2.7$ and $R_{\nu\nu} < 3.9$, both at 90% C.L. [77].

4.2.7 $b\bar{b} \rightarrow \mu^+\mu^-$ scattering

The measurements of $\mu^+\mu^-$ spectra at high invariant mass $m_{\mu\mu}$ are sensitive to large couplings $y_{s\mu}$ or $y_{b\mu}$. The relevant channel in our case is $b\bar{b} \rightarrow \mu^+\mu^-$ which directly limits $y_{b\mu}$. If we assume that effective dim-6 operator description is a good approximation to the t -channel S_3 exchange at LHC energy, then we can use a 1σ bound derived in Ref. [78]

$$y_{b\mu}^2 < 0.30(m_{S_3}/\text{TeV})^2. \tag{4.25}$$

4.2.8 D decays

The weak triplet nature of S_3 implies couplings only to the weak doublets of quarks and leptons, and thus corrections to the charged current processes only rescale the SM charged current contributions. The dominant modification of V_{cs} element associated with semi-muonic decays follows from Eq. (3.2):

$$V_{cs} \rightarrow V_{cs} - \frac{v^2}{4m_{S_3}^2} (y_{s\mu} + V_{cb}^* y_{b\mu}) y_{s\mu}. \quad (\text{for processes with } \mu\bar{\nu}_\mu). \tag{4.26}$$

Assuming that the CKM-suppressed $y_{b\mu}$ term can be neglected in Eq. (4.26) and using the fact that current precision on the semileptonically determined V_{cs} reaches 1 per-mille [60], we find $y_{s\mu} \lesssim 0.3(m_{S_3}/\text{TeV})$.

Rare charm decays with two leptons, e.g. $D^0 \rightarrow \mu^+\mu^-$ and $D \rightarrow M\mu^+\mu^-$, are most constraining at the moment (for dineutrino modes cf. [79]), where M can be a pseudoscalar or a vector meson. The effective Wilson coefficient of the left-handed current, $C_9 = -C_{10} \approx (V_{us}\pi v^2)/(\alpha V_{ub}V_{cb}^* m_{S_3}^2) y_{s\mu}^2$ can be compared to the bounds, $|C_9|, |C_{10}| \lesssim 1.0/|V_{ub}V_{cb}|$, obtained in Ref. [80]. We learn that the ensuing bound $y_{s\mu} \lesssim 0.5(m_{S_3}/\text{TeV})$ from rare decays is weaker than the abovementioned bound from semileptonic decays.

5 Flavor couplings

In this section we study three scenarios differing in the number of variable Yukawas. For each scenario we report a minimum of χ^2 function, which is a sum of terms corresponding to all observables discussed in the preceding sections. We also report 1σ regions for the

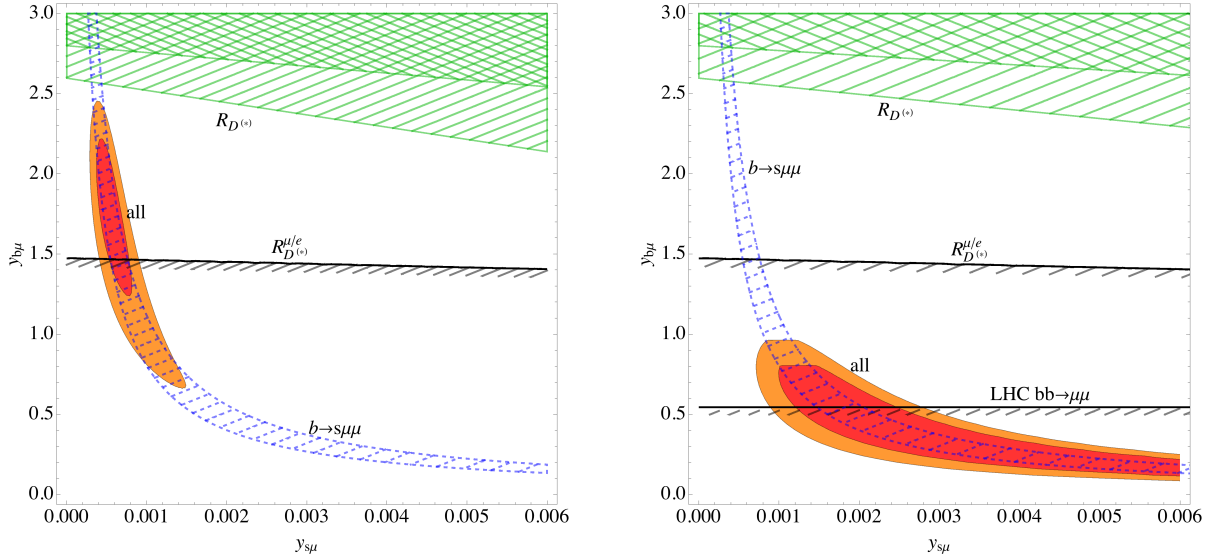


Figure 2. Left panel: $R_{D^{(*)}}$ is resolved in hatched (2σ) and doubly hatched (1σ) regions, whereas the $b \rightarrow s\mu\mu$ puzzle is resolved in dashed-hatched region at 1σ . Region below the black line with a hatching is in 1σ agreement with $R_{D^{(*)}}^{\mu/e}$. No LHC constraint on $y_{b\mu}$ is considered. Right panel: Same as left panel apart from inclusion of constraint on $y_{b\mu}$ from LHC. Red and orange regions in both graphs denote 1σ and 2σ results of the fit.

interesting two-dimensional projections of parameter space. While performing these fits we limit all free Yukawa couplings to be smaller than 3. Introduction of this artificial cut-off is guided by the constraints posed by the LHC searches, discussed in Sec. 6. The SM point has $\chi^2 = 71.6$ and serves as a reference value to which χ^2 of the three fits are compared.

5.1 S_3 coupled to muons (2 parameters)

In this scenario we consider only the effect of S_3 with non-zero muonic couplings:

$$y = \begin{pmatrix} 0 & 0 & 0 \\ 0 & y_{s\mu} & 0 \\ 0 & y_{b\mu} & 0 \end{pmatrix}. \quad (5.1)$$

We set $m_{S_3} = 1$ TeV and for the moment ignore the direct LHC constraint on $y_{b\mu}$ spelled out in Eq. (4.25). In this case the best fit point has $\chi^2 = 34.7$ reached at $y_{s\mu} = 5 \times 10^{-4}$ and $y_{b\mu} = 1.8$. The $R_{D^{(*)}}$ puzzle can be addressed by lowering $\mathcal{B}(B \rightarrow D^{(*)}\mu\nu)$ which requires large $y_{b\mu}$ coupling as seen in Eq. (3.4). The 1σ and 2σ regions of the fit are shown in Fig. 2. Left panel in Fig. 2 exposes tension between $R_{D^{(*)}}$ (2.8σ pull) and $R_{D^{(*)}}^{\mu/e}$ (1.8σ pull) which is even more exacerbated when we include the direct constraints on $y_{b\mu}$ from LHC (right panel of Fig. 2). The latter scenario with all constraints included has $\chi^2 = 42.4$ at point $(y_{s\mu}, y_{b\mu}) = \pm(2 \times 10^{-3}, 0.46)$ which corresponds to the 5.0σ pull of the SM hypothesis. One can observe in the right panel in Fig. 2 that in this case the preferred region is drawn further away from $R_{D^{(*)}}$. The results indicate that $R_{D^{(*)}}$ cannot be explained by omitting couplings to τ . Detailed results on the pulls are given in the third column of Tab. 1.

	SM	$m_{S_3} = 1 \text{ TeV}$ ($y_{s\mu}, y_{b\mu}$) w.o./w. Eq. (4.25)	$m_{S_3} = 1.0/1.5 \text{ TeV}$ ($y_{s\mu}, y_{b\mu}, y_{s\tau}, y_{b\tau}$)	Eq.
χ^2	71.6	34.7/42.4	36.8/38.0	
$b \rightarrow s\ell^+\ell^-$	5.4	0.0/0.0	0.0/0.0	(3.8)
$R_{D^{(*)}}$	4.5	2.8/4.4	4.0/4.2	(3.4)
$(g-2)_\mu$	3.1	3.5/3.1	3.1/3.1	(4.15)
$R_{\tau/\mu}^K$	2.0	2.0/2.0	0.3/0.3	(4.7)
$R_{\tau/e}^{\tau}$	2.0	1.6/2.0	2.1/2.1	(4.10)
$\mathcal{B}(B \rightarrow \tau\nu)$	1.2	1.2/1.2	1.1/1.2	(4.2)
Δm_s	1.1	1.1/1.1	1.6/1.6	(4.19)
$R_{e/\mu}^K$	1.1	1.1/1.1	1.1/1.1	(4.5)
$R_{\tau/\mu}^{\mu}$	0.7	0.7/0.7	0.8/0.8	(4.10)
$R_{D^{(*)}}^{\mu/e}$	0.5	1.8/0.4	0.5/0.5	(4.1)
$R_{\nu\nu}$	0.5	0.6/0.6	0.8/0.6	(4.24)
$b\bar{b} \rightarrow \mu\mu$	0.0	-/0.7	0.0/0.0	(4.25)
$\mathcal{B}(\tau \rightarrow \mu\gamma)$	0.0	0.0/0.0	0.4/0.3	(4.11)
$\mathcal{B}(B \rightarrow K\tau\mu)$	0.0	0.0/0.0	0.3/0.3	(4.16)

Table 1. Observables that enter the global fit with their pulls in σ in the SM and S_3 scenarios. Third column represents the case when $m_{S_3} = 1 \text{ TeV}$ and only $y_{s\mu}, y_{b\mu}$ are allowed, without/with taking into account $b\bar{b} \rightarrow \mu\mu$ constraint. Fourth column represents the fit of the $y_{s\mu}, y_{b\mu}, y_{s\tau}, y_{b\tau}$ scenario for $m_{S_3} = 1.0/1.5 \text{ TeV}$. The constraints with negligible pulls are not shown in this table.

5.2 S_3 coupled to muons and taus (4 parameters)

Since the purely muonic couplings are in conflict with $R_{D^{(*)}}$ we allow in addition for tauonic couplings of S_3 :

$$y = \begin{pmatrix} 0 & 0 & 0 \\ 0 & y_{s\mu} & y_{s\tau} \\ 0 & y_{b\mu} & y_{b\tau} \end{pmatrix}. \quad (5.2)$$

In this case both couplings with the muons tend to be small, below 0.1, and are relevant only in $b \rightarrow s\mu\mu$, whereas the couplings to τ are ~ 1 in order to enhance $R_{D^{(*)}}$. For $m_{S_3} = 1 \text{ TeV}$ we find that the minimal χ^2 of this scenario with 4 degrees of freedom is 36.8 reached at $(y_{s\mu}, y_{b\mu}, y_{s\tau}, y_{b\tau}) = (0.047, 0.020, 0.87, -0.048)$ ⁵ which makes the SM point excluded at 5.0σ (pull). In Fig. 3 the fit in the tauonic couplings' plane shows how the optimal region is still far from the central value of $R_{D^{(*)}}$, mostly due to $R_{\nu\nu}$ and Δm_s , which do not allow for large products of $y_{b\tau}y_{s\tau}$. Pulls of individual observables for $m_{S_3} = 1.0/1.5 \text{ TeV}$ are presented in the fourth column of Table 1.

⁵The fit is approximately invariant with respect to the overall sign of the muonic or tauonic couplings which implies a fourfold degeneracy.

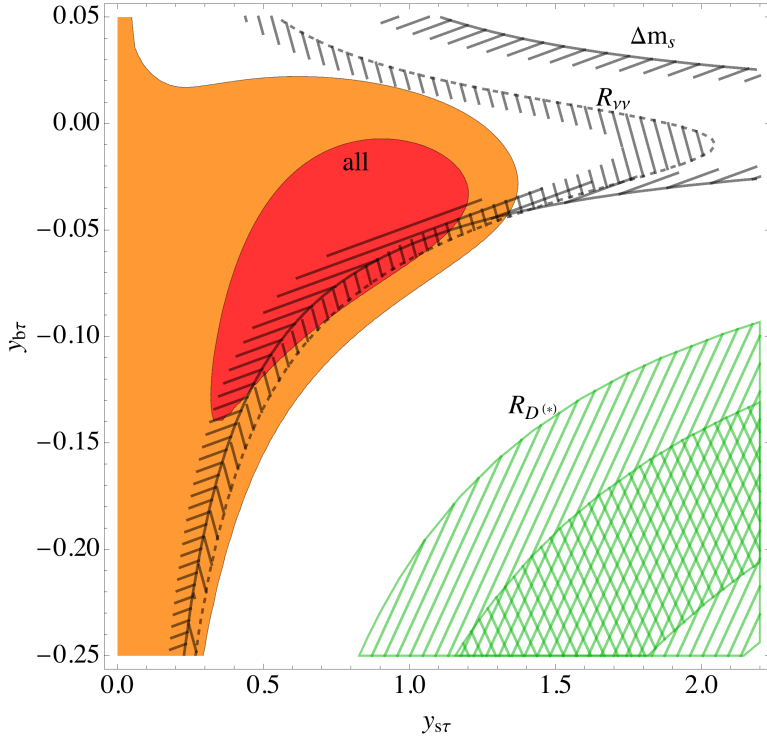


Figure 3. Fit for the $m_{S_3} = 1$ TeV scenario with four free couplings. $R_{D^{(*)}}$ is resolved within hatched (2σ) and doubly hatched (1σ) regions. Region to the left of the dashed line (hatched) is in 1σ agreement with $R_{\nu\nu}$ and $R_{\nu\nu}^*$. Δm_s prefers (at 2σ) a region on the hatched side of full line. Red and orange regions are 1σ and 2σ results of the fit.

5.3 S_3 and \tilde{R}_2 (6 parameters)

In order to relax the tension in the $y_{s\tau}$ - $y_{b\tau}$ plane between large effect in $R_{D^{(*)}}$ and well constrained $R_{\nu\nu}^{(*)}$ and Δm_s , we could invoke a light \tilde{R}_2 with couplings to τ . We consider a case $m_{S_3} = m_{\tilde{R}_2} = 1$ TeV with six free Yukawa couplings (y_{ij} from the previous subsection and $(\tilde{y}_{s\tau}, \tilde{y}_{b\tau})$ pair) to find $\chi^2 = 33.4$ at $(y_{s\mu}, y_{b\mu}, y_{s\tau}, y_{b\tau}) = (0.051, 0.019, 0.86, -0.069)$, $(\tilde{y}_{s\tau}, \tilde{y}_{b\tau}) = (3, 0.0026)$ ⁶ that represents a 4.9σ pull of the SM. Most importantly, the tension in $R_{D^{(*)}}$ is only marginally improved and stands at 3.7σ . The presence of \tilde{R}_2 allows for partial cancellation in Δm_s between large tauonic couplings of S_3 and \tilde{R}_2 , which is not the case in both $R_{\nu\nu}$ and $R_{\nu\nu}^*$, where cancellation in one observable necessary spoils the other (cf. (4.24)). We thus conclude that light \tilde{R}_2 with relatively large couplings to the SM fermions cannot improve substantially the agreement with data. We accordingly assume that the couplings of \tilde{R}_2 , i.e., \tilde{y}_{ij} of Eq. (2.3), are small enough as not to affect flavor observables. With light \tilde{R}_2 and its Yukawa couplings sufficiently small to avoid flavor constraints we can still aid gauge coupling unification and generate viable neutrino masses in the underlying GUT model as we show in Sec. 7.

⁶Degenerate best-fit points are obtained by flipping sign of individual Yukawas in a manner that does not change signs of $y_{s\mu}y_{b\mu}$, $y_{s\tau}y_{b\tau}$, $\tilde{y}_{s\tau}\tilde{y}_{b\tau}$, and $y_{s\tau}\tilde{y}_{s\tau}$.

6 Collider constraints

In what follows we confront our model, comprising two light LQs, with collider constraints while taking into account the particularities of the flavor structure derived in the previous section. We demonstrate the viability of the proposed model and present bounds from third generation LQ pair production as well as high-mass $\tau\tau$ production searches at the 13 TeV LHC for current and projected luminosities. We show that a large portion of the relevant parameter space can be covered by the HL-LHC.

6.1 LQ pair production

The current best mass limit for LQs that decay to the third-generation leptons has been recently reported by the CMS Collaboration while searching for a pair of QCD produced LQs decaying into the $\tau^+\tau^-b\bar{b}$ channel [81]. This search excludes an LQ with mass below 850 GeV (550 GeV) for a branching ratio (BR) of $\beta = 1$ ($\beta = 0.5$). This search can set limits on the parameter space of our model via $pp \rightarrow S_3^{4/3*} S_3^{4/3} (\tilde{R}_2^{2/3*} \tilde{R}_2^{2/3}) \rightarrow \tau^+\tau^-b\bar{b}$ processes.

We focus on the scenario presented in Sec. 5.2 when S_3 is at the TeV scale and \tilde{R}_2 is assumed not to feed significantly in the $\tau^+\tau^-b\bar{b}$ signal. In this case the CMS bound can be applied directly to the $S_3^{4/3}$ state, at a benchmark mass of $m_{S_3} = 1$ TeV, decaying into a τb pair with a BR given by

$$\beta \approx \frac{|y_{b\tau}|^2}{|y_{b\tau}|^2 + |y_{s\tau}|^2}. \quad (6.1)$$

Here we neglect the small widths of $S_3^{4/3}$ into both muonic channels. Results are given in Fig. 4 (left panel), where the dashed blue contours represent the 95% C.L. exclusion limits for different LHC luminosities and the red region represents the 1σ region for the

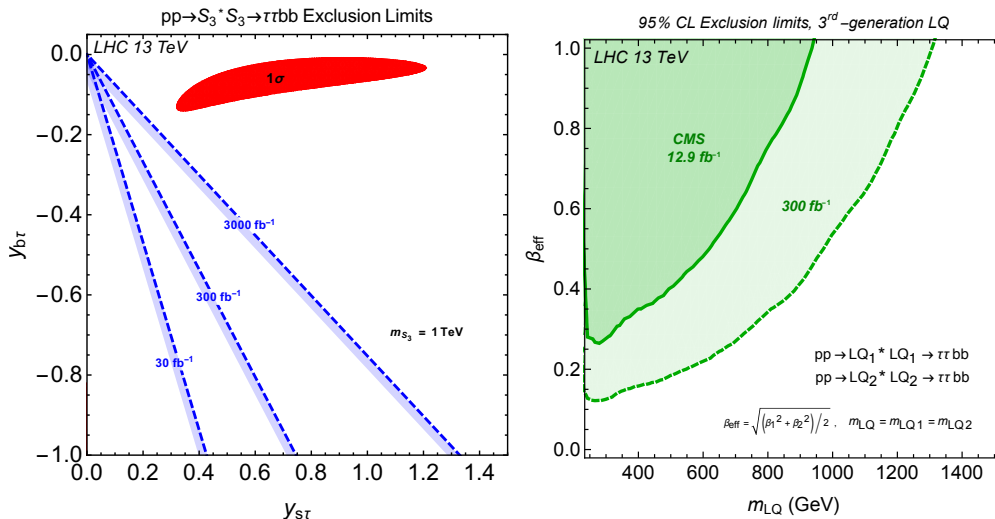


Figure 4. (Left Panel) 95% C.L. exclusion limits from LQ pair production (dotted blue lines) at different projected LHC luminosities for a 1 TeV S_3 LQ. The red region corresponds to the 1σ low energy fit. (Right panel) Reinterpretation of the CMS Collaboration exclusion limits for two generic degenerate LQs decaying into $\tau\tau bb$ final state in the $\beta_{\text{eff}}-m_{\text{LQ}}$ plane.

low-energy fit derived in Sec. 5.2. It is worth mentioning that we did not include other contributions which could potentially tighten these bounds, for example, contributions from $pp \rightarrow S_3^{4/3*} S_3^{4/3} \rightarrow \tau^+ \tau^- b s$.⁷ The search starts losing sensitivity for m_{S_3} above 1 TeV, while for masses larger than 1.2 TeV the search does not produce any useful limits. In conclusion, a third generation LQ pair production search at the LHC is not a sensitive probe for this particular flavor structure of our LQ model.

We now turn to the scenario where two generic third generation LQs (like e.g. S_3 and \tilde{R}_2) are at the TeV scale and both contribute to LQ pair production. A naive reinterpretation of the CMS limits [81] can be performed when (i) both LQ components are degenerate in mass⁸, (ii) interference terms between the final state τb pairs at the amplitude level are negligible and, (iii) the LQ decay widths are small enough in order to guarantee the narrow width approximation (NWA) assumed in the experimental search. This scenario would thus correspond to the particular case we investigated in Sec. 5.3.

As shown in Appendix A, the CMS bound for one LQ can be directly mapped into a bound for two degenerate LQs we denote with LQ_1 and LQ_2 , for simplicity, when the associated BRs are β_1 and β_2 , respectively. (See Fig. 2 (right panel) of Ref. [81] for the experimental limit.) The inferred limits, which apply in general to two third-generation LQs with non-interfering final states, are presented in Fig. 4 (right panel) for an integrated luminosity of 12.9 fb^{-1} (solid green contour). For example, we find that both LQs with equal masses below 930 GeV (600 GeV) are excluded at 95% C.L. if $\beta_{\text{eff}} = 1$ ($\beta_{\text{eff}} = 0.5$), where $\beta_{\text{eff}} = \sqrt{(\beta_1^2 + \beta_2^2)/2}$. We also include LHC projections for an integrated luminosity of 300 fb^{-1} (dashed green contour) by rescaling the CMS Collaboration limits with the square root of the luminosity ratio. At this projected luminosity the LQ pair production search is not sensitive for masses above 1.3 TeV. These results, again, can be used for our LQ model for degenerate S_3 and \tilde{R}_2 LQs at the TeV scale. Unfortunately, the LHC bounds on the couplings extracted from LQ pair production search are not strong enough to probe this scenario either.

6.2 High-mass $\tau\tau$ production

In this section we study the implication of light S_3 and \tilde{R}_2 leptoquarks for high- p_T $\tau\tau$ production at the LHC. It was shown in Refs. [32, 82] that $\tau\tau$ resonance searches at the LHC produce stringent constraints on a large class of models explaining the $R_{D^{(*)}}$ anomaly. In what follows we give predictions for the deviation from the SM in the invariant mass tails of $pp \rightarrow \tau^+ \tau^-$ and derive bounds at different luminosities for the parameter space of the present LQ model from the 13 TeV ATLAS Collaboration resonance search at 3.2 fb^{-1} [83].

Both LQs contribute to $pp \rightarrow \tau^+ \tau^-$ production exclusively through Yukawa interactions by exchanging $S_3^{4/3}$, $S_3^{1/3}$, and $\tilde{R}_2^{2/3}$ components in the t -channel from partonic $q\bar{q}$ annihilation. The relevant Feynman diagrams are depicted in Fig. 5. Potentially large

⁷This process will produce events in the signal region defined in Ref. [81], which is based on only one b -tagged jet and not two. We have also excluded from our analysis contributions coming from the non-QCD LQ pair production.

⁸For the non-degenerate case the results of Ref. [81] are not directly applicable given that each LQ will have different kinematic distributions leading to different selection efficiencies in the signal region.

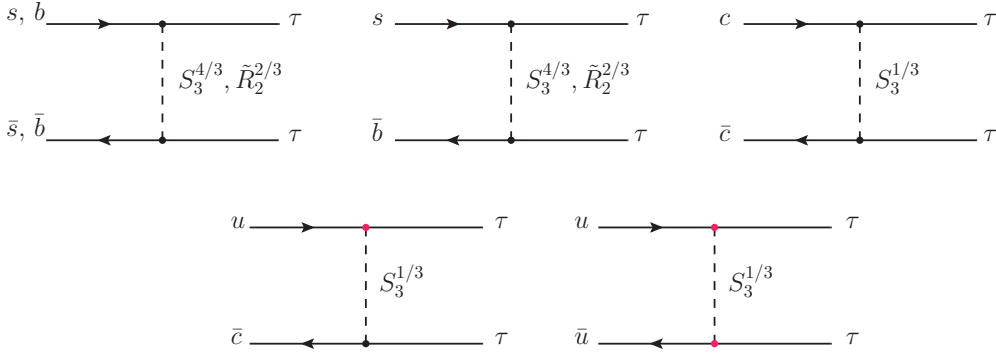


Figure 5. Leading order Feynman diagrams for the t -channel S_3 and \tilde{R}_2 exchanges in $pp \rightarrow \tau^+\tau^-$ process. The red vertex indicates the presence of the $|V_{us}|$ Cabibbo suppression in the coupling.

contributions may come from the processes with incoming strange quarks $s\bar{s} \rightarrow \tau^+\tau^-$ and $s\bar{b} (b\bar{s}) \rightarrow \tau^+\tau^-$, followed by sub-leading contributions from bottom, charm and up quark initiated processes $b\bar{b} (c\bar{c}) (u\bar{u}) \rightarrow \tau^+\tau^-$. The flavor structure in Eq. (2.2) also allows for $S_3^{1/3}$ to couple to u and τ via the CKM mixing. Nevertheless, this coupling is proportional to $|V_{us}|y_{s\tau}$, meaning that $\tau\tau$ production from incoming up quarks is Cabibbo suppressed leading to negligible cross-sections of order $|V_{us}|^2$ and $|V_{us}|^4$ for the processes $c\bar{u} \rightarrow \tau^+\tau^-$ and $u\bar{u} \rightarrow \tau^+\tau^-$, respectively. The Cabibbo suppressed vertices are shown in red in Feynman diagrams of Fig. 5. On the other hand, at high- x the large proton PDF of the valence up quark in the process $u\bar{c} \rightarrow \tau^+\tau^-$ can marginally compensate for the $|V_{us}|$ suppression in the amplitude giving a contribution comparable to $c\bar{c} \rightarrow \tau^+\tau^-$ in the total cross-section.

We now focus on the total cross-section $\sigma_{\text{TOT}}^{\text{fid}}$ of $pp \rightarrow \tau^+\tau^-$ far from the Z -pole in the high-mass tails of the $\tau\tau$ invariant mass distribution. We will, for definiteness, study the scenario where only S_3 contributes to $\tau\tau$ production. The couplings of \tilde{R}_2 are assumed to be small and can thus be safely neglected for this collider study. This is in accordance with the outcome of the numerical study presented in Sec. 5.2.

At leading-order (LO), $\tau\tau$ production will receive contributions from the t -channel exchange of S_3 , from the s -channel SM Drell-Yan $pp \rightarrow Z/\gamma^* \rightarrow \tau\tau$ production, and from interference effects between these processes. The high-mass kinematic region is defined by the following fiducial cuts on the final states: $p_T > 100$ GeV (50 GeV) for the leading (sub-leading) τ and a high invariant mass cut for the $\tau\tau$ pair of $m_{\tau\tau} > 600$ GeV. We define the *signal strength* $\mu_{pp \rightarrow \tau\tau}$ as the ratio of $\sigma_{\text{TOT}}^{\text{fid}}$ with the the SM Drell-Yan fiducial cross-section $\sigma_{\text{SM}}^{\text{fid}}$:

$$\mu_{pp \rightarrow \tau\tau} \equiv \sigma_{\text{TOT}}^{\text{fid}} / \sigma_{\text{SM}}^{\text{fid}} = 1 + \sigma_{\text{LQ}}^{\text{fid}} / \sigma_{\text{SM}}^{\text{fid}}. \quad (6.2)$$

Here the fiducial cross-section $\sigma_{\text{LQ}}^{\text{fid}}$ includes all NP contributions from both the LQ squared and LQ-SM interference amplitudes, i.e., $\sigma_{\text{LQ}}^{\text{fid}} = 2 \text{Re}(\mathcal{A}_{\text{SM}}^* \mathcal{A}_{\text{LQ}}) + |\mathcal{A}_{\text{LQ}}|^2$. The ratio $\sigma_{\text{LQ}}^{\text{fid}} / \sigma_{\text{SM}}^{\text{fid}}$ quantifies the NP deviation of the total fiducial cross-section from the expected SM prediction. The LQ Yukawa couplings enter in $\sigma_{\text{LQ}}^{\text{fid}}$ as

$$\sigma_{\text{LQ}}^{\text{fid}}(y_{s\tau}, y_{b\tau}) = \sigma_{s\bar{s}}(y_{s\tau}) + \sigma_{s\bar{b}}(y_{s\tau}, y_{b\tau}) + \sigma_{b\bar{b}}(y_{b\tau}) + \sigma_{c\bar{c}, u\bar{u}, u\bar{c}}(y_{s\tau}), \quad (6.3)$$

In order to conform with the analysis in Sec. 5 we assume all Yukawa couplings to be real. Here $\sigma_{s\bar{s}}$, $\sigma_{s\bar{b}}$, $\sigma_{b\bar{b}}$ and $\sigma_{c\bar{c}, u\bar{u}, u\bar{c}}$ correspond to the fiducial cross-sections of the processes $s\bar{s} \rightarrow \tau^+\tau^-$, $s\bar{b}(\bar{s}b) \rightarrow \tau^+\tau^-$, $b\bar{b} \rightarrow \tau^+\tau^-$ and $c\bar{c}(u\bar{u})(u\bar{c}) \rightarrow \tau^+\tau^-$ respectively. These can be expressed as generic quartic polynomials in the couplings:

$$\sigma_{s\bar{s}}(y_{s\tau}) = y_{s\tau}^4 A_1 + y_{s\tau}^2 B_1, \quad (6.4)$$

$$\sigma_{s\bar{b}}(y_{s\tau}, y_{b\tau}) = y_{s\tau}^2 y_{b\tau}^2 A_2, \quad (6.5)$$

$$\sigma_{b\bar{b}}(y_{b\tau}) = y_{b\tau}^4 A_3 + y_{b\tau}^2 B_3, \quad (6.6)$$

$$\sigma_{c\bar{c}, u\bar{u}, u\bar{c}}(y_{s\tau}) = y_{s\tau}^4 A_4 - y_{s\tau}^2 B_4. \quad (6.7)$$

The polynomial coefficients A_i and B_i are functions of the mass m_{S_3} describing the LQ squared amplitudes and LQ-SM interference amplitudes, respectively. In Eqs. (6.4)–(6.7) we define all polynomial coefficients to be positive and include the explicit signs of the LQ-SM interference coefficients B_i , indicating the presence of either destructive or constructive interference amplitudes. The origin of the sign of these interference terms can be traced back to the SM amplitude proportional to the $T_3 - \sin^2\theta_W Q$ coupling of the Z boson with the incoming quarks along with the sign of the LQ Yukawa interactions of $S_3^{4/3(1/3)}$. The interference arising between the Z boson and the $S_3^{4/3(1/3)}$ components is driven by the weak isospin of the quark doublets, i.e., positive (negative) for up(down)-type quarks. This translates into a constructive interference for down-type quarks in $d\bar{d}, s\bar{s}, b\bar{b} \rightarrow \tau\tau$ processes and destructive interference for up-type quarks in $c\bar{c}, u\bar{u} \rightarrow \tau\tau$ processes. As a

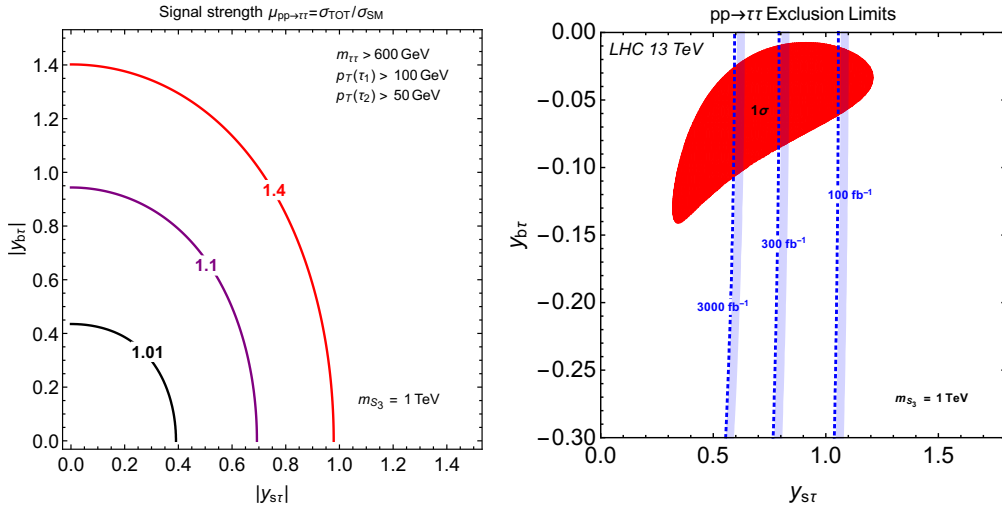


Figure 6. (Left panel) Contours of constant signal strength $\mu_{pp \rightarrow \tau\tau}$ for different deviations from the SM prediction at $m_{S_3} = 1 \text{ TeV}$. (Right panel) 95% C.L. limits for LHC luminosities of 100, 300, and, 3000 fb^{-1} (dotted blue contours) from recasting high-mass $\tau\tau$ searches by ATLAS [83] for $m_{S_3} = 1 \text{ TeV}$. The red region corresponds to the 1 σ low-energy fit.

consequence, this relative sign that appears between the LQ-SM interferences in different $\tau\tau$ production channels leads to a partial cancellation in the cross-section $\sigma_{\text{LQ}}^{\text{fid}}$. For more details see Appendix B.

For the calculations below we choose a benchmark mass value of 1 TeV. In order to extract the values of the polynomial coefficients A_i and B_i we generate in `FeynRules` [84] the UFO model file for the Lagrangian for S_3 and simulate in `MadGraph5` [85] 13 TeV event samples of $pp \rightarrow \tau^+\tau^-$ subject to the high-mass fiducial cuts discussed above for different values of the couplings. The specific values of the coefficients can be found in Appendix B. In Fig. 6 (left panel) we show results for different contours of constant signal strength $\mu_{pp \rightarrow \tau\tau}$ in the $y_{s\tau}-y_{b\tau}$ plane for the 1 TeV mass scenario. This shows that our LQ model equipped with the proposed flavor structure with $y_{s\tau, b\tau}$ couplings of $\mathcal{O}(1)$, predicts at the LHC an enhancement of $\mathcal{O}(10\%)$ in the $\tau\tau$ tails when compared to the SM.

In the remaining part of this section we confront our model with existing LHC data and extract 95% C.L. limits for the model parameters at different integrated luminosities. For this we recast a heavy Z' search by the ATLAS Collaboration with 3.2 fb^{-1} of data in the fully hadronic $\tau_{\text{had}}\tau_{\text{had}}$ channel [83]. For the recast we generate at LO in `MadGraph5` a set of the LQ $\tau_{\text{had}}\tau_{\text{had}}$ signal samples followed by parton showering and hadronization in `Pythia8` [86]. We have included interference effects between the LQ signals and the SM Drell-Yan background process. Detector effects are simulated in `Delphes3` [87] with settings tuned according to the experimental environment of the $\tau_{\text{had}}\tau_{\text{had}}$ inclusive category as described in Ref. [83]. For this category, events are selected if the reconstructed objects satisfies the following requirements:

- $p_T > 110 \text{ GeV}$ (55 GeV) for the leading (sub-leading) τ_{had} .
- Events with isolated electrons (muons) are vetoed if $p_T > 10 \text{ GeV}$ ($p_T > 15 \text{ GeV}$).
- Opposite sign $\tau_{\text{had}}\tau_{\text{had}}$ with back-to-back topology in the transverse plane, $\Delta\phi(\tau_{\text{had}}\tau_{\text{had}}) > 2.7$.
- Total transverse mass cut of $m_T^{\text{tot}} > 350 \text{ GeV}$.

Here m_T^{tot} is the dynamical variable used to reconstruct the invariant mass of the visible part of $\tau_{\text{had}}\tau_{\text{had}}$ defined as $(m_T^{\text{tot}})^2 \equiv m_T^2(\tau_1, \tau_2) + m_T^2(\tau_1, E_T^{\text{miss}}) + m_T^2(\tau_2, E_T^{\text{miss}})$ where E_T^{miss} is the total missing energy in the event and $m_T^2(A, B) = p_T(A)p_T(B)(1 - \cos\Delta\phi(A, B))$ is the squared transverse mass of objects A and B . In order to extract limits from the tails of the m_T^{tot} distributions we use the statistical analysis presented in Ref. [82]. For $m_{\text{LQ}} > 1 \text{ TeV}$ the most sensitive bin corresponds to the last one ($m_T^{\text{tot}} > 684 \text{ GeV}$) where a point in parameter space is excluded at 95% C.L. if the number of events in that bin exceeds 11, 36 and 113 at integrated luminosities of 30, 300, 3000 fb^{-1} respectively. Here we have applied a naive scaling of the limits for the 3.2 fb^{-1} search to arbitrary luminosities with $\sqrt{\mathcal{L}_{\text{int}}/3.2 \text{ fb}^{-1}}$. The results are given in Fig. 6 (Right panel) for the benchmark mass of $m_{\text{LQ}} = 1 \text{ TeV}$. There the regions to the right of the dotted blue boundaries are excluded at 95% C.L. for future LHC luminosities of 30 fb^{-1} , 300 fb^{-1} and 3000 fb^{-1} . In the plot we have also included the 1σ region in solid red obtained from the low-energy fit to all flavor

experiments performed in Sec. 5.2. Notice that these bounds are conservative given that we have not included NLO QCD corrections and have not taken into account other processes such as non-resonant $qg \rightarrow \tau\tau q$ that can produce sizeable contributions to the inclusive $\tau_{\text{had}}\tau_{\text{had}}$ category⁹. From these results we conclude that the High-Luminosity LHC can probe a large portion of the parameter space for the Yukawa coupling ansatz of Sec. 5.2.

7 GUT completion

The preceding sections were devoted to the study of the impact of light scalar fields S_3 and \tilde{R}_2 with potentially sizeable couplings to the quark-lepton pairs on the flavor physics processes and LHC observables. Here we want to demonstrate that these fields and associated couplings can originate from a consistent grand unified theory (GUT) model.

To insure that the LHC accessible leptiquarks S_3 and \tilde{R}_2 are not in conflict with stringent limits on matter stability it is necessary that both S_3 and \tilde{R}_2 do not couple to the quark-quark pairs either directly or through the mixing with other scalars in a specific model of unification. It turns out that one can meet this requirement in an $SU(5)$ model that comprises 5-, 15-, 24-, and 45-dimensional scalar representations [52]. The decomposition of the scalar sector of that model is $\mathbf{5} = (\Psi_D, \Psi_T) = (\mathbf{1}, \mathbf{2}, 1/2) \oplus (\mathbf{3}, \mathbf{1}, -1/3)$, $\mathbf{15} = (\Phi_a, \Phi_b, \Phi_c) = (\mathbf{1}, \mathbf{3}, 1) \oplus (\mathbf{3}, \mathbf{2}, 1/6) \oplus (\mathbf{6}, \mathbf{1}, -2/3)$, $\mathbf{24} = (\Sigma_8, \Sigma_3, \Sigma_{(3,2)}, \Sigma_{(\bar{3},2)}, \Sigma_{24}) = (\mathbf{8}, \mathbf{1}, 0) \oplus (\mathbf{1}, \mathbf{3}, 0) \oplus (\mathbf{3}, \mathbf{2}, -5/6) \oplus (\bar{\mathbf{3}}, \mathbf{2}, 5/6) \oplus (\mathbf{1}, \mathbf{1}, 0)$, and $\mathbf{45} = (\Delta_1, \Delta_2, \Delta_3, \Delta_4, \Delta_5, \Delta_6, \Delta_7) = (\mathbf{8}, \mathbf{2}, 1/2) \oplus (\bar{\mathbf{6}}, \mathbf{1}, -1/3) \oplus (\mathbf{3}, \mathbf{3}, -1/3) \oplus (\bar{\mathbf{3}}, \mathbf{2}, -7/6) \oplus (\mathbf{3}, \mathbf{1}, -1/3) \oplus (\bar{\mathbf{3}}, \mathbf{1}, 4/3) \oplus (\mathbf{1}, \mathbf{2}, 1/2)$, where Φ_b and Δ_3 are identified with \tilde{R}_2 and S_3^* , respectively. The fermions of the SM, on the other hand, are embedded within the tenplets and fiveplets in the usual manner [88].

We first show that this GUT scenario is compatible with the viable gauge coupling unification. To this end, we take all scalar fields in the model that mediate proton decay at tree-level to reside at or above 10^{12} GeV. These fields are Ψ_T , Δ_5 , and Δ_6 [52]. We furthermore set the masses of both S_3 and \tilde{R}_2 at 1 TeV and constrain all remaining scalar fields to be at or above one scale we simply denote m that is to be determined through the requirement that the gauge coupling unification takes place at the one-loop level. Note that Σ_{24} does not affect unification. Also, $\Sigma_{(3,2)}$ and $\Sigma_{(\bar{3},2)}$ are not physical fields since they provide necessary degrees of freedom for the baryon and lepton number violating gauge bosons X and Y of the $SU(5)$ origin to become massive fields.

The gauge couplings meet at the unification scale m_{GUT} when the following equation is satisfied [89]

$$\frac{B_{23}}{B_{12}} = \frac{5 \sin^2 \theta_W - \alpha/\alpha_S}{8 \cdot 3/8 - \sin^2 \theta_W} = 0.721 \pm 0.004, \quad (7.1)$$

where the right-hand side is evaluated using $\alpha_S(m_Z) = 0.1193 \pm 0.0016$, $\alpha^{-1}(m_Z) = 127.906 \pm 0.019$, and $\sin^2 \theta_W = 0.23126 \pm 0.00005$ [90]. The left-hand side depends on the particle content and the mass spectrum of the model. Namely, coefficients B_{ij} are $B_{ij} = \sum_J (b_i^J - b_j^J) r_J$, where b_i^J are the well-known β -function coefficients of particle J with

⁹This last process, although α_s suppressed, has a large PDF from the initial gluon that enhances the total inclusive cross-section by $\mathcal{O}(10\%)$ or more.

mass m_J and $r_J = (\ln m_{\text{GUT}}/m_J)/(\ln m_{\text{GUT}}/m_Z)$. The sum goes through all particles beside the SM ones that reside between Z boson mass m_Z and m_{GUT} . The convention is such that b_1^J , b_2^J , and b_3^J are associated with $U(1)$, $SU(2)$, and $SU(3)$ of the SM, respectively. We identify m_{GUT} not only with the gauge coupling unification scale but with the masses of the proton decay mediating gauge boson fields X and Y .

If and when unification takes place for a given m we evaluate m_{GUT} using equation [89]

$$\ln \frac{m_{\text{GUT}}}{m_Z} = \frac{16\pi}{5\alpha} \frac{3/8 - \sin^2 \theta_W}{B_{12}} = \frac{184.8 \pm 0.1}{B_{12}} \quad (7.2)$$

to check that $m_{\text{GUT}} \geq 5 \times 10^{15}$ GeV in order to satisfy stringent bounds on the X and Y gauge boson mediated proton decay. To actually set a lower bound on m we fix $m_{\text{GUT}} = 5 \times 10^{15}$ GeV in our analysis and maximise m . We find that $m = 3.1 \times 10^{10}$ GeV when the masses of both \tilde{R}_2 and S_3 are at 1 TeV. The masses of all other scalar particles in the model are $m_{\Psi_D} = 10^2$ GeV, $m_{\Psi_T} = 10^{12}$ GeV, $m_{\Phi_a} = m_{\text{GUT}}$, $m_{\Phi_c} = m$, $m_{\Sigma_8} = m$, $m_{\Sigma_3} = m_{\text{GUT}}$, $m_{\Delta_1} = m$, $m_{\Delta_2} = m$, $m_{\Delta_4} = 1.2 \times 10^{12}$ GeV, $m_{\Delta_5} = 10^{12}$ GeV, and $m_{\Delta_6} = 10^{12}$ GeV, $m_{\Delta_7} = m_{\text{GUT}}$. Note that the SM Higgs is in principle a mixture of Ψ_T and Δ_7 . We accordingly take one state to be light and treat the mass of the other as a free parameter that is between m and m_{GUT} .

The fact that viable unification can take place when S_3 and \tilde{R}_2 are both light does not come as a surprise. Note that the SM field content yields $B_{23}^{\text{SM}}/B_{12}^{\text{SM}} = 0.53$ instead of the experimentally required value given in Eq. (7.1). The nice feature of the set-up with light S_3 and \tilde{R}_2 is that both fields have positive b_{23}^J and negative b_{12}^J coefficients. This not only helps in bringing the left-hand side of Eq. (7.1) in agreement with the required experimental value but simultaneously raises the GUT scale m_{GUT} through Eq. (7.2). The relevant coefficients are $b_{23}^{S_3} = 9/6$, $b_{12}^{S_3} = -27/15$, $b_{23}^{\tilde{R}_2} = 1/6$, and $b_{12}^{\tilde{R}_2} = -7/15$. Again, our findings demonstrate that the gauge coupling unification is possible for light S_3 and \tilde{R}_2 in this particular model.

We next demonstrate that the explicit forms of the Yukawa couplings of S_3 and \tilde{R}_2 that are used in Sec. 5 to produce numerical fits can originate from the appropriate $SU(5)$ operators. It is also argued that the model can accommodate realistic masses of the SM fermions.

The $S_3 \in \overline{\mathbf{45}}$ lepton-quark couplings originate from the $SU(5)$ contraction $y_{ij}^{45} \mathbf{10}_i \bar{\mathbf{5}}_j \overline{\mathbf{45}}$, where $\mathbf{10}_i$ are the usual fermionic tenplets, $i(= 1, 2, 3)$ is the generation index, and y^{45} is a 3×3 matrix in flavor space. We can thus identify y of Eq. (2.1) with $y^{45}/\sqrt{2}$, where y^{45} is related to the difference in masses between charged fermions and down-type quarks [52]. This follows from the fact that there are actually two operators that contribute towards the charged fermion and down-type quark masses in this $SU(5)$ model [91]. One is $y_{ij}^{45} \mathbf{10}_i \bar{\mathbf{5}}_j \overline{\mathbf{45}}$ and the other is $y_{ij}^5 \mathbf{10}_i \bar{\mathbf{5}}_j \bar{\mathbf{5}}$, where y^5 is an arbitrary complex matrix. Clearly, $y^{45} = \sqrt{2}y$ and y^5 together contain enough parameters to easily address observed mismatch between the charged fermion and down-type quark masses. For completeness we specify that the up-type quark masses originate from a single contraction $x_{ij} \mathbf{10}_i \mathbf{10}_j \mathbf{5}$, where x_{ij} is a symmetric complex 3×3 matrix.

The $\tilde{R}_2 \in \mathbf{15}$ lepton-quark couplings are symmetric in flavor space since they originate from $y_{ij}^{15} \bar{\mathbf{5}}_i \bar{\mathbf{5}}_j \mathbf{15}$, where $\bar{\mathbf{5}}_i$ are the usual fermionic fiveplets. We identify \tilde{y}_{ij} of Eq. (2.3) with $-(D_R y^{15})_{ij}/\sqrt{2}$ in the physical basis for the down-type quarks and charged leptons, where D_R represents unitary transformation of the right-chiral down-type quarks. If we take that $y_{33}^{15} \neq 0$ we obtain the form of \tilde{y} that is used in the fit of Sec. 5 when we consider joint effect of S_3 and \tilde{R}_2 on flavor observables.

It is worth mentioning that it is possible to address neutrino masses within this model. Namely, if one turns on a vacuum expectation value of the electrically neutral field $\Phi_a \in \mathbf{15}$ one can generate neutrino masses of Majorana nature via type II see-saw mechanism [92, 93] through the same operator that yields the \tilde{R}_2 lepton-quark couplings, i.e., $y_{ij}^{15} \bar{\mathbf{5}}_i \bar{\mathbf{5}}_j \mathbf{15}$. In this particular instance the entries in y^{15} would need to be responsible for the observed mass-squared differences and mixing angles in the neutrino sector. That requirement would not be compatible with a simple ansatz for the structure of \tilde{y} given in Eq. (2.4). Again, viable neutrino masses would only be possible if we depart from that ansatz and assume that the \tilde{y}_{ij} entries are sufficiently small to avoid flavor constraints for light \tilde{R}_2 . This is in agreement with the findings we presented in Sec. 5.3. Note that the neutrino Majorana masses could also receive partial contribution through the one-loop processes, where the particles in the loop are down-quarks and a mixture of S_3 and \tilde{R}_2 [52, 94, 95].

The preceding discussion demonstrates that the $SU(5)$ GUT model comprising 5-, 15-, 24-, and 45-dimensional scalar representations, with the canonical embedding of the SM fermions, can accommodate light S_3 and \tilde{R}_2 and describe observed fermion masses of the SM without any conflict with relevant experimental constraints.

8 Conclusion

Our aim, in the present work, is to accommodate the observed lepton non-universality in charged current processes, signalled by $R_{D^{(*)}}$, as well as lepton non-universality and the global tension in the $b \rightarrow s\mu^+\mu^-$ sector through the introduction of light scalar LQ S_3 . This LQ emerges naturally in the context of a specific $SU(5)$ GUT model and has to be accompanied by another light scalar LQ \tilde{R}_2 which improves gauge coupling unification and aids neutrino mass generation.

The first state, S_3 , couples left-handed s and b to left-handed μ and τ and is capable of accommodating $b \rightarrow s\ell^+\ell^-$ sector. Because of its weak triplet nature it also couples to up-type quarks and neutrinos which are precisely the additional couplings needed to address $R_{D^{(*)}}$. Large couplings needed for $R_{D^{(*)}}$ cause the weak triplet S_3 to inevitably contribute to other well constrained flavor observables that agree with the SM predictions. We have analyzed those in detail and demonstrated that the most pressing ones, $R_{\nu\nu}^{(*)} = \mathcal{B}(B \rightarrow K^{(*)}\bar{\nu}\nu)/\mathcal{B}(B \rightarrow K^{(*)}\bar{\nu}\nu)_{\text{SM}}$ and Δm_s , allow only for minor improvement of $R_{D^{(*)}}$ puzzle. We furthermore show that the second state, \tilde{R}_2 , cannot significantly improve the agreement with data.

Based on the numerical values of the LQ Yukawa couplings as obtained in the flavor fit we recast two LQ collider searches: (i) search for pair produced LQs decaying to $b\tau b\tau$, (ii) search for high-mass $\tau\tau$ final state which is sensitive to the t -channel LQ exchange.

From the recast of the search for the LQ pair production we find that the proposed scenario with $m_{S_3} = 1 \text{ TeV}$ cannot be significantly probed in a large portion of the parameter space even with 300 fb^{-1} of integrated luminosity at the Large Hadron Collider. Complementary searches for $\tau\tau$ final states produced via a single LQ exchange, on the other hand, are not as hampered by large LQ masses and are already excluding corners of the parameter space with largest individual Yukawa couplings. Moreover, since the flavor fit requires increasing Yukawa couplings for larger LQ masses the sensitivity of high-mass $\tau\tau$ final state search does not degrade at higher masses as compared to the pair production mechanism. This method can probe almost entire parameter space of the model at 3000 fb^{-1} of integrated luminosity.

A natural ultraviolet completion for the two LQ states is an $SU(5)$ GUT. We demonstrate that a particular setting with 5-, 15-, 24-, and 45-dimensional scalar representations is consistent with unification of the gauge couplings, where light S_3 and \tilde{R}_2 leptoquarks reside in 45- and 15-dimensional representations, respectively. Furthermore, baryon number violation is sufficiently suppressed by lack of diquark couplings of S_3 and high enough scale of the rest of the GUT spectrum. The model also accommodates the masses of all fermions of the SM.

Acknowledgments

We thank J.F. Kamenik and M. Nardecchia for insightful discussions. N.K. would like to thank B. Capdevila and S. Descotes-Genon for kindly providing results of the global fit of $b \rightarrow s\mu\mu$ in the scenario with two leptoquarks. This work has been supported in part by Croatian Science Foundation under the project 7118. S.F. and N.K. acknowledge support of the Slovenian Research Agency through research core funding No. P1-0035. I.D. acknowledges support of COST Action CA15108. D.A.F. acknowledges support by the ‘Young Researchers Programme’ of the Slovenian Research Agency.

A LQ pair production recast

In this appendix we give a reinterpretation of the results by the CMS Collaboration [81] for the case of two LQs, denoted LQ_1 and LQ_2 . When addressing the LQ pair production from QCD interactions, a model with two LQs of degenerate mass $m_{LQ} \equiv m_{LQ_1} = m_{LQ_2}$ with BRs β_1 and β_2 for $LQ_1 \rightarrow \tau b$ and $LQ_2 \rightarrow \tau b$, respectively, can be consistently mapped to a model with only one LQ, denoted here as LQ, with an *effective* mass m_{eff} and an *effective* BR β_{eff} for $LQ \rightarrow \tau b$. In this case, assuming the NWA, the total cross-section for $pp \rightarrow LQ^*LQ \rightarrow \tau^+\tau^-b\bar{b}$ is factorized into production and decay modes as

$$\sigma_{pp \rightarrow \tau\tau bb} = \beta_{\text{eff}}^2 \times \sigma_{\text{pair}}(m_{\text{eff}}), \quad (\text{A.1})$$

where σ_{pair} is the $pp \rightarrow LQ^*LQ$ pair production cross-section that depends exclusively on the LQ mass when only QCD interactions are taken into account. For the numerical

calculations we use the approximate expression from Ref. [96] for the cross-section at NLO

$$\sigma_{\text{pair}}(m) \approx \exp \left\{ \sum_{n=-2}^2 C_n \left(\frac{m}{[\text{TeV}]} \right)^n \right\} [\text{fb}], \quad (\text{A.2})$$

where $(C_{-2}, C_{-1}, C_0, C_1, C_2) = (-0.300, 3.318, 2.762, -3.780, -0.299)$ at NLO in QCD for LHC collision energies of $\sqrt{s} = 13$ TeV. Equating the right hand side of Eq. (A.1) to the total cross-section derived in the two LQ scenario $\sigma_{pp \rightarrow \tau\tau bb} = (\beta_1^2 + \beta_2^2) \sigma_{\text{pair}}(m_{\text{LQ}})$ and demanding $0 \leq \beta_{\text{eff}} \leq 1$ we find

$$\beta_{\text{eff}} = \sqrt{\frac{\beta_1^2 + \beta_2^2}{2}}, \quad m_{\text{eff}} = \sigma^{-1}(2 \sigma_{\text{pair}}(m_{\text{LQ}})), \quad (\text{A.3})$$

where σ^{-1} is the inverse function of Eq. (A.2). Here we assume negligible interference effects between the decay products of the $\text{LQ}_{1,2}$ and simply add two cross-sections together. After calculating σ^{-1} numerically we can use Eq. (A.3) to map the CMS Collaboration 12.9 fb^{-1} exclusion limits in the β - m_{LQ} plane as reported in Fig. 9 of Ref. [81] into the exclusion limits for two generic non-interfering third-generation LQs with degenerate mass. These limits are shown in Fig. 4.

B High-mass $\tau\tau$ production cross-sections

We obtain the following fiducial cross-sections in fb for the process $pp \rightarrow \tau\tau$ for $m_{\text{LQ}} = 1$ TeV:

$$\sigma_{s\bar{s}}(y_{s\tau}) = 12.042 y_{st}^4 + 5.126 y_{st}^2, \quad (\text{B.1})$$

$$\sigma_{s\bar{b}}(y_{s\tau}, y_{b\tau}) = 12.568 y_{st}^2 y_{b\tau}^2, \quad (\text{B.2})$$

$$\sigma_{b\bar{b}}(y_{b\tau}) = 3.199 y_{b\tau}^4 + 1.385 y_{b\tau}^2, \quad (\text{B.3})$$

$$\sigma_{c\bar{c}, u\bar{u}, u\bar{c}}(y_{s\tau}) = 3.987 y_{st}^4 - 5.189 y_{st}^2. \quad (\text{B.4})$$

Notice that in each individual production channel the interferences can be large. In particular, these dominate in $c\bar{c}(u\bar{u})(u\bar{c}) \rightarrow \tau\tau$ production over the squared LQ terms for Yukawa couplings of order one, as shown in Eq. (B.4). Only after summing across all channels the total interference is found to be sub-leading when compared to the total LQ squared amplitudes in most portions of parameter space. This happens because of an accidental cancellation between the constructive S_3 - Z interference in $s\bar{s} \rightarrow \tau\tau$ given by the second term in Eq. (B.1) and the destructive S_3 - Z interference in $c\bar{c}(u\bar{u})(u\bar{c}) \rightarrow \tau\tau$ given by the second term in Eq. (B.4). The remaining small (constructive) interference after cancellations is mostly given by $\tau\tau$ production from bottom fusion and is negligible in high-mass $\tau\tau$ searches for the current level of experimental uncertainties.

References

- [1] BABAR collaboration, J. P. Lees et al., *Evidence for an excess of $\bar{B} \rightarrow D^{(*)} \tau^- \bar{\nu}_\tau$ decays*, *Phys. Rev. Lett.* **109** (2012) 101802, [1205.5442].

- [2] BABAR collaboration, J. P. Lees et al., *Measurement of an Excess of $\bar{B} \rightarrow D^{(*)}\tau^-\bar{\nu}_\tau$ Decays and Implications for Charged Higgs Bosons*, *Phys. Rev.* **D88** (2013) 072012, [[1303.0571](#)].
- [3] BELLE collaboration, M. Huschle et al., *Measurement of the branching ratio of $\bar{B} \rightarrow D^{(*)}\tau^-\bar{\nu}_\tau$ relative to $\bar{B} \rightarrow D^{(*)}\ell^-\bar{\nu}_\ell$ decays with hadronic tagging at Belle*, *Phys. Rev.* **D92** (2015) 072014, [[1507.03233](#)].
- [4] BELLE collaboration, I. Adachi et al., *Measurement of $B \rightarrow D^{(*)}\tau\nu$ using full reconstruction tags*, in *Proceedings, 24th International Symposium on Lepton-Photon Interactions at High Energy (LP09): Hamburg, Germany, August 17-22, 2009*, 2009, [0910.4301](#), <https://inspirehep.net/record/834881/files/arXiv:0910.4301.pdf>.
- [5] BELLE collaboration, A. Bozek et al., *Observation of $B^+ \rightarrow \bar{D}^{*0}\tau^+\nu_\tau$ and Evidence for $B^+ \rightarrow \bar{D}^0\tau^+\nu_\tau$ at Belle*, *Phys. Rev.* **D82** (2010) 072005, [[1005.2302](#)].
- [6] LHCb collaboration, R. Aaij et al., *Measurement of the ratio of branching fractions $\mathcal{B}(\bar{B}^0 \rightarrow D^{*+}\tau^-\bar{\nu}_\tau)/\mathcal{B}(\bar{B}^0 \rightarrow D^{*+}\mu^-\bar{\nu}_\mu)$* , *Phys. Rev. Lett.* **115** (2015) 111803, [[1506.08614](#)].
- [7] BELLE collaboration, S. Hirose et al., *Measurement of the τ lepton polarization and $R(D^*)$ in the decay $\bar{B} \rightarrow D^*\tau^-\bar{\nu}_\tau$* , *Phys. Rev. Lett.* **118** (2017) 211801, [[1612.00529](#)].
- [8] D. Bečirević, S. Fajfer, N. Košnik and O. Sumensari, *Leptoquark model to explain the B -physics anomalies, R_K and R_D* , *Phys. Rev.* **D94** (2016) 115021, [[1608.08501](#)].
- [9] D. Bigi and P. Gambino, *Revisiting $B \rightarrow D\ell\nu$* , *Phys. Rev.* **D94** (2016) 094008, [[1606.08030](#)].
- [10] Y. Amhis et al., *Averages of b -hadron, c -hadron, and τ -lepton properties as of summer 2016*, [1612.07233](#).
- [11] S. Fajfer, J. F. Kamenik, I. Nisandzic and J. Zupan, *Implications of Lepton Flavor Universality Violations in B Decays*, *Phys. Rev. Lett.* **109** (2012) 161801, [[1206.1872](#)].
- [12] Z. Ligeti, M. Papucci and D. J. Robinson, *New Physics in the Visible Final States of $B \rightarrow D^{(*)}\tau\nu$* , *JHEP* **01** (2017) 083, [[1610.02045](#)].
- [13] A. Crivellin, J. Fuentes-Martin, A. Greljo and G. Isidori, *Lepton Flavor Non-Universality in B decays from Dynamical Yukawas*, *Phys. Lett.* **B766** (2017) 77–85, [[1611.02703](#)].
- [14] W. Altmannshofer, P. S. B. Dev and A. Soni, *$R_{D^{(*)}}$ anomaly: A possible hint for natural supersymmetry with R -parity violation*, [1704.06659](#).
- [15] R. Alonso, B. Grinstein and J. Martin Camalich, *Lifetime of B_c^- Constrains Explanations for Anomalies in $B \rightarrow D^{(*)}\tau\nu$* , *Phys. Rev. Lett.* **118** (2017) 081802, [[1611.06676](#)].
- [16] A. Crivellin and S. Pokorski, *Can the differences in the determinations of V_{ub} and V_{cb} be explained by New Physics?*, *Phys. Rev. Lett.* **114** (2015) 011802, [[1407.1320](#)].
- [17] B. Bhattacharya, A. Datta, D. London and S. Shivashankara, *Simultaneous Explanation of the R_K and $R(D^{(*)})$ Puzzles*, *Phys. Lett.* **B742** (2015) 370–374, [[1412.7164](#)].
- [18] S. Bhattacharya, S. Nandi and S. K. Patra, *Optimal-observable analysis of possible new physics in $B \rightarrow D^{(*)}\tau\nu$* , *Phys. Rev.* **D93** (2016) 034011, [[1509.07259](#)].
- [19] C. Hati, G. Kumar and N. Mahajan, *$\bar{B} \rightarrow D^{(*)}\tau\bar{\nu}$ excesses in ALRSM constrained from B , D decays and $D^0 - \bar{D}^0$ mixing*, *JHEP* **01** (2016) 117, [[1511.03290](#)].
- [20] Y. Sakaki, M. Tanaka, A. Tayduganov and R. Watanabe, *Probing New Physics with q^2 distributions in $\bar{B} \rightarrow D^{(*)}\tau\bar{\nu}$* , *Phys. Rev.* **D91** (2015) 114028, [[1412.3761](#)].

- [21] B. Capdevila, S. Descotes-Genon, L. Hofer and J. Matias, *Hadronic uncertainties in $B \rightarrow K^* \mu^+ \mu^-$: a state-of-the-art analysis*, *JHEP* **04** (2017) 016, [[1701.08672](#)].
- [22] LHCb collaboration, R. Aaij et al., *Test of lepton universality using $B^+ \rightarrow K^+ \ell^+ \ell^-$ decays*, *Phys. Rev. Lett.* **113** (2014) 151601, [[1406.6482](#)].
- [23] LHCb collaboration, R. Aaij et al., *Test of lepton universality with $B^0 \rightarrow K^{*0} \ell^+ \ell^-$ decays*, [1705.05802](#).
- [24] M. Bordone, G. Isidori and A. Pattori, *On the Standard Model predictions for R_K and R_{K^*}* , *Eur. Phys. J.* **C76** (2016) 440, [[1605.07633](#)].
- [25] G. Hiller and F. Kruger, *More model-independent analysis of $b \rightarrow s$ processes*, *Phys. Rev.* **D69** (2004) 074020, [[hep-ph/0310219](#)].
- [26] BELLE collaboration, S. Wehle et al., *Lepton-Flavor-Dependent Angular Analysis of $B \rightarrow K^* \ell^+ \ell^-$* , *Phys. Rev. Lett.* **118** (2017) 111801, [[1612.05014](#)].
- [27] W. Altmannshofer, S. Gori, M. Pospelov and I. Yavin, *Quark flavor transitions in $L_\mu - L_\tau$ models*, *Phys. Rev.* **D89** (2014) 095033, [[1403.1269](#)].
- [28] A. Datta, M. Duraisamy and D. Ghosh, *Explaining the $B \rightarrow K^* \mu^+ \mu^-$ data with scalar interactions*, *Phys. Rev.* **D89** (2014) 071501, [[1310.1937](#)].
- [29] G. Hiller and M. Schmaltz, *R_K and future $b \rightarrow s \ell \ell$ physics beyond the standard model opportunities*, *Phys. Rev.* **D90** (2014) 054014, [[1408.1627](#)].
- [30] S. L. Glashow, D. Guadagnoli and K. Lane, *Lepton Flavor Violation in B Decays?*, *Phys. Rev. Lett.* **114** (2015) 091801, [[1411.0565](#)].
- [31] B. Gripaios, M. Nardecchia and S. A. Renner, *Composite leptoquarks and anomalies in B -meson decays*, *JHEP* **05** (2015) 006, [[1412.1791](#)].
- [32] A. Greljo, G. Isidori and D. Marzocca, *On the breaking of Lepton Flavor Universality in B decays*, *JHEP* **07** (2015) 142, [[1506.01705](#)].
- [33] D. Ghosh, M. Nardecchia and S. A. Renner, *Hint of Lepton Flavour Non-Universality in B Meson Decays*, *JHEP* **12** (2014) 131, [[1408.4097](#)].
- [34] A. Crivellin, G. D'Ambrosio and J. Heeck, *Explaining $h \rightarrow \mu^\pm \tau^\mp$, $B \rightarrow K^* \mu^+ \mu^-$ and $B \rightarrow K \mu^+ \mu^- / B \rightarrow K e^+ e^-$ in a two-Higgs-doublet model with gauged $L_\mu - L_\tau$* , *Phys. Rev. Lett.* **114** (2015) 151801, [[1501.00993](#)].
- [35] A. Crivellin, G. D'Ambrosio and J. Heeck, *Addressing the LHC flavor anomalies with horizontal gauge symmetries*, *Phys. Rev.* **D91** (2015) 075006, [[1503.03477](#)].
- [36] A. Crivellin, D. Müller and T. Ota, *Simultaneous Explanation of $R(D^{(*)})$ and $b \rightarrow s \mu^+ \mu^-$: The Last Scalar Leptoquarks Standing*, [1703.09226](#).
- [37] D. Aristizabal Sierra, F. Staub and A. Vicente, *Shedding light on the $b \rightarrow s$ anomalies with a dark sector*, *Phys. Rev.* **D92** (2015) 015001, [[1503.06077](#)].
- [38] I. de Medeiros Varzielas and G. Hiller, *Clues for flavor from rare lepton and quark decays*, *JHEP* **06** (2015) 072, [[1503.01084](#)].
- [39] A. Crivellin, L. Hofer, J. Matias, U. Nierste, S. Pokorski and J. Rosiek, *Lepton-flavour violating B decays in generic Z' models*, *Phys. Rev.* **D92** (2015) 054013, [[1504.07928](#)].
- [40] A. Celis, J. Fuentes-Martin, M. Jung and H. Serodio, *Family nonuniversal Z' models with protected flavor-changing interactions*, *Phys. Rev.* **D92** (2015) 015007, [[1505.03079](#)].

- [41] M. Freytsis, Z. Ligeti and J. T. Ruderman, *Flavor models for $\bar{B} \rightarrow D^{(*)}\tau\bar{\nu}$* , *Phys. Rev.* **D92** (2015) 054018, [[1506.08896](#)].
- [42] S. Fajfer and N. Košnik, *Vector leptoquark resolution of R_K and $R_{D^{(*)}}$ puzzles*, *Phys. Lett.* **B755** (2016) 270–274, [[1511.06024](#)].
- [43] P. Cox, A. Kusenko, O. Sumensari and T. T. Yanagida, *$SU(5)$ Unification with TeV-scale Leptoquarks*, *JHEP* **03** (2017) 035, [[1612.03923](#)].
- [44] D. Bečirević and O. Sumensari, *A leptoquark model to accommodate $R_K^{\text{exp}} < R_K^{\text{SM}}$ and $R_{K^*}^{\text{exp}} < R_{K^*}^{\text{SM}}$* , [1704.05835](#).
- [45] J. F. Kamenik, Y. Soreq and J. Zupan, *Lepton flavor universality violation without new sources of quark flavor violation*, [1704.06005](#).
- [46] P. Arnan, D. Bečirević, F. Mescia and O. Sumensari, *Two Higgs Doublet Models and $b \rightarrow s$ exclusive decays*, [1703.03426](#).
- [47] D. Ghosh, *Explaining the R_K and R_{K^*} anomalies*, [1704.06240](#).
- [48] D. Bardhan, P. Byakti and D. Ghosh, *A closer look at the R_D and R_{D^*} anomalies*, *JHEP* **01** (2017) 125, [[1610.03038](#)].
- [49] B. Capdevila, A. Crivellin, S. Descotes-Genon, J. Matias and J. Virto, *Patterns of New Physics in $b \rightarrow s\ell^+\ell^-$ transitions in the light of recent data*, [1704.05340](#).
- [50] L. Calibbi, A. Crivellin and T. Ota, *Effective Field Theory Approach to $b \rightarrow s\ell\ell^{(\prime)}$, $B \rightarrow K^{(*)}\nu\bar{\nu}$ and $B \rightarrow D^{(*)}\tau\nu$ with Third Generation Couplings*, *Phys. Rev. Lett.* **115** (2015) 181801, [[1506.02661](#)].
- [51] I. Doršner, S. Fajfer, A. Greljo, J. F. Kamenik and N. Košnik, *Physics of leptoquarks in precision experiments and at particle colliders*, *Phys. Rept.* **641** (2016) 1–68, [[1603.04993](#)].
- [52] I. Doršner, S. Fajfer and N. Košnik, *Leptoquark mechanism of neutrino masses within the grand unification framework*, *Eur. Phys. J.* **C77** (2017) 417, [[1701.08322](#)].
- [53] R. Alonso, B. Grinstein and J. Martin Camalich, *Lepton universality violation and lepton flavor conservation in B-meson decays*, *JHEP* **10** (2015) 184, [[1505.05164](#)].
- [54] F. Feruglio, P. Paradisi and A. Pattori, *On the Importance of Electroweak Corrections for B Anomalies*, [1705.00929](#).
- [55] F. Feruglio, P. Paradisi and A. Pattori, *Revisiting Lepton Flavor Universality in B Decays*, *Phys. Rev. Lett.* **118** (2017) 011801, [[1606.00524](#)].
- [56] D. Bečirević, S. Fajfer and N. Košnik, *Lepton flavor nonuniversality in $b \rightarrow s\ell^+\ell^-$ processes*, *Phys. Rev.* **D92** (2015) 014016, [[1503.09024](#)].
- [57] S. Descotes-Genon, L. Hofer, J. Matias and J. Virto, *Global analysis of $b \rightarrow s\ell\ell$ anomalies*, *JHEP* **06** (2016) 092, [[1510.04239](#)].
- [58] BELLE collaboration, A. Abdesselam et al., *Precise determination of the CKM matrix element $|V_{cb}|$ with $\bar{B}^0 \rightarrow D^{*+}\ell^-\bar{\nu}_\ell$ decays with hadronic tagging at Belle*, [1702.01521](#).
- [59] BELLE collaboration, R. Glattauer et al., *Measurement of the decay $B \rightarrow D\ell\nu_\ell$ in fully reconstructed events and determination of the Cabibbo-Kobayashi-Maskawa matrix element $|V_{cb}|$* , *Phys. Rev.* **D93** (2016) 032006, [[1510.03657](#)].
- [60] PARTICLE DATA GROUP collaboration, C. Patrignani et al., *Review of Particle Physics*, *Chin. Phys.* **C40** (2016) 100001.

- [61] V. Cirigliano and I. Rosell, *Two-loop effective theory analysis of $\pi(K) \rightarrow e\bar{\nu}_e[\gamma]$ branching ratios*, *Phys. Rev. Lett.* **99** (2007) 231801, [[0707.3439](#)].
- [62] A. Pich, *Precision Tau Physics*, *Prog. Part. Nucl. Phys.* **75** (2014) 41–85, [[1310.7922](#)].
- [63] R. Decker and M. Finkemeier, *Short and long distance effects in the decay $\tau \rightarrow \pi\nu_\tau(\gamma)$* , *Nucl. Phys.* **B438** (1995) 17–53, [[hep-ph/9403385](#)].
- [64] CDF collaboration, T. A. Aaltonen et al., *Study of Top-Quark Production and Decays involving a Tau Lepton at CDF and Limits on a Charged-Higgs Boson Contribution*, *Phys. Rev.* **D89** (2014) 091101, [[1402.6728](#)].
- [65] BABAR collaboration, B. Aubert et al., *Searches for Lepton Flavor Violation in the Decays $\tau^\pm \rightarrow e^\pm\gamma$ and $\tau^\pm \rightarrow \mu^\pm\gamma$* , *Phys. Rev. Lett.* **104** (2010) 021802, [[0908.2381](#)].
- [66] I. Doršner, S. Fajfer, N. Košnik and I. Nišandžić, *Minimally flavored colored scalar in $\bar{B} \rightarrow D^{(*)}\tau\bar{\nu}$ and the mass matrices constraints*, *JHEP* **11** (2013) 084, [[1306.6493](#)].
- [67] F. S. Queiroz, K. Sinha and A. Strumia, *Leptoquarks, Dark Matter, and Anomalous LHC Events*, *Phys. Rev.* **D91** (2015) 035006, [[1409.6301](#)].
- [68] BABAR collaboration, J. P. Lees et al., *A search for the decay modes $B^{+-} \rightarrow h^{+-}\tau^{+}l$* , *Phys. Rev.* **D86** (2012) 012004, [[1204.2852](#)].
- [69] J. A. Bailey et al., *$B \rightarrow Kl^{+}l^{-}$ decay form factors from three-flavor lattice QCD*, *Phys. Rev.* **D93** (2016) 025026, [[1509.06235](#)].
- [70] F. Gabbiani, E. Gabrielli, A. Masiero and L. Silvestrini, *A Complete analysis of FCNC and CP constraints in general SUSY extensions of the standard model*, *Nucl. Phys.* **B477** (1996) 321–352, [[hep-ph/9604387](#)].
- [71] A. J. Buras, M. Jamin and P. H. Weisz, *Leading and Next-to-leading QCD Corrections to ϵ Parameter and $B^0 - \bar{B}^0$ Mixing in the Presence of a Heavy Top Quark*, *Nucl. Phys.* **B347** (1990) 491–536.
- [72] FERMILAB LATTICE, MILC collaboration, A. Bazavov et al., *$B_{(s)}^0$ -mixing matrix elements from lattice QCD for the Standard Model and beyond*, *Phys. Rev.* **D93** (2016) 113016, [[1602.03560](#)].
- [73] S. Aoki et al., *Review of lattice results concerning low-energy particle physics*, *Eur. Phys. J.* **C77** (2017) 112, [[1607.00299](#)].
- [74] S. Fajfer, J. F. Kamenik and N. Kosnik, *$b \rightarrow dd\bar{s}$ transition and constraints on new physics in B^- decays*, *Phys. Rev.* **D74** (2006) 034027, [[hep-ph/0605260](#)].
- [75] W. Altmannshofer, A. J. Buras, D. M. Straub and M. Wick, *New strategies for New Physics search in $B \rightarrow K^*\nu\bar{\nu}$, $B \rightarrow K\nu\bar{\nu}$ and $B \rightarrow X_s\nu\bar{\nu}$ decays*, *JHEP* **04** (2009) 022, [[0902.0160](#)].
- [76] A. J. Buras, J. Girrbach-Noe, C. Niehoff and D. M. Straub, *$B \rightarrow K^{(*)}\nu\bar{\nu}$ decays in the Standard Model and beyond*, *JHEP* **02** (2015) 184, [[1409.4557](#)].
- [77] BELLE collaboration, J. Grygier et al., *Search for $B \rightarrow h\nu\bar{\nu}$ decays with semileptonic tagging at Belle*, [[1702.03224](#)].
- [78] A. Greljo and D. Marzocca, *High- p_T dilepton tails and flavor physics*, *Eur. Phys. J.* **C77** (2017) 548, [[1704.09015](#)].
- [79] S. de Boer and G. Hiller, *Flavor and new physics opportunities with rare charm decays into leptons*, *Phys. Rev.* **D93** (2016) 074001, [[1510.00311](#)].

- [80] S. Fajfer and N. Košnik, *Prospects of discovering new physics in rare charm decays*, *Eur. Phys. J. C* **75** (2015) 567, [[1510.00965](#)].
- [81] CMS collaboration, A. M. Sirunyan et al., *Search for the third-generation scalar leptoquarks and heavy right-handed neutrinos in final states with two tau leptons and two jets in proton-proton collisions at $\sqrt{s} = 13$ TeV*, [1703.03995](#).
- [82] D. A. Faroughy, A. Greljo and J. F. Kamenik, *Confronting lepton flavor universality violation in B decays with high- p_T tau lepton searches at LHC*, *Phys. Lett. B* **764** (2017) 126–134, [[1609.07138](#)].
- [83] ATLAS collaboration, M. Aaboud et al., *Search for Minimal Supersymmetric Standard Model Higgs bosons H/A and for a Z' boson in the $\tau\tau$ final state produced in pp collisions at $\sqrt{s} = 13$ TeV with the ATLAS Detector*, *Eur. Phys. J. C* **76** (2016) 585, [[1608.00890](#)].
- [84] A. Alloul, N. D. Christensen, C. Degrande, C. Duhr and B. Fuks, *FeynRules 2.0 - A complete toolbox for tree-level phenomenology*, *Comput. Phys. Commun.* **185** (2014) 2250–2300, [[1310.1921](#)].
- [85] J. Alwall, R. Frederix, S. Frixione, V. Hirschi, F. Maltoni, O. Mattelaer et al., *The automated computation of tree-level and next-to-leading order differential cross sections, and their matching to parton shower simulations*, *JHEP* **07** (2014) 079, [[1405.0301](#)].
- [86] T. Sjöstrand, S. Ask, J. R. Christiansen, R. Corke, N. Desai, P. Ilten et al., *An Introduction to PYTHIA 8.2*, *Comput. Phys. Commun.* **191** (2015) 159–177, [[1410.3012](#)].
- [87] DELPHES 3 collaboration, J. de Favereau, C. Delaere, P. Demin, A. Giammanco, V. Lemaitre, A. Mertens et al., *DELPHES 3, A modular framework for fast simulation of a generic collider experiment*, *JHEP* **02** (2014) 057, [[1307.6346](#)].
- [88] H. Georgi and S. L. Glashow, *Unity of All Elementary Particle Forces*, *Phys. Rev. Lett.* **32** (1974) 438–441.
- [89] A. Giveon, L. J. Hall and U. Sarid, *$SU(5)$ unification revisited*, *Phys. Lett. B* **271** (1991) 138–144.
- [90] PARTICLE DATA GROUP collaboration, K. A. Olive et al., *Review of Particle Physics*, *Chin. Phys. C* **38** (2014) 090001.
- [91] H. Georgi and C. Jarlskog, *A New Lepton - Quark Mass Relation in a Unified Theory*, *Phys. Lett. B* **86B** (1979) 297–300.
- [92] G. Lazarides, Q. Shafi and C. Wetterich, *Proton Lifetime and Fermion Masses in an $SO(10)$ Model*, *Nucl. Phys. B* **181** (1981) 287–300.
- [93] R. N. Mohapatra and G. Senjanovic, *Neutrino Masses and Mixings in Gauge Models with Spontaneous Parity Violation*, *Phys. Rev. D* **23** (1981) 165.
- [94] C.-K. Chua, X.-G. He and W.-Y. P. Hwang, *Neutrino mass induced radiatively by supersymmetric leptoquarks*, *Phys. Lett. B* **479** (2000) 224–229, [[hep-ph/9905340](#)].
- [95] U. Mahanta, *Neutrino masses and mixing angles from leptoquark interactions*, *Phys. Rev. D* **62** (2000) 073009, [[hep-ph/9909518](#)].
- [96] T. Mandal, S. Mitra and S. Seth, *Pair Production of Scalar Leptoquarks at the LHC to NLO Parton Shower Accuracy*, *Phys. Rev. D* **93** (2016) 035018, [[1506.07369](#)].